Damage assessment and collapse investigation of three historical masonry palaces under seismic actions

by
Marco VALENTE[(1)], Gabriele MILANI[*(1)]

(1) Department of Architecture, Built Environment and Construction Engineering
Politecnico di Milano, Piazza Leonardo da Vinci 32, 20133 Milano, Italy
** Corresponding author. E-mail: gabriele.milani@polimi.it*
Phone: +39 022399 4290 Fax: +39 022399 4220

Abstract

The preservation (in terms of inhibition of failures and collapses) of architectural heritage against horizontal loads (such as earthquakes) requires an accurate assessment of the non-linear response up to failure: to this aim, the use of advanced numerical tools to perform three-dimensional non-linear dynamic analyses is fundamental. This paper investigates the performance (up to the activation of local failures and under horizontal loads) of three historical masonry palaces of the outstanding cultural heritage in Mantua (Northern Italy) after the 2012 Emilia earthquake. Despite the unquestionable importance of the three case studies, until now these palaces have not been studied with advanced numerical simulations; moreover, the recent seismic sequence and the consequent significant cracks patterns observed in the post-earthquake survey phase have pointed out their vulnerability even to small seismic actions. The first part of the study was addressed to an accurate knowledge of the three palaces, focusing especially on the information gathered during on-site surveys, bibliographical and historical research: the data collected were employed to detect the complex three-dimensional geometry of the palaces under study and to define the cracks patterns. In the second part of the study, detailed and representative three-dimensional finite element (FE) models of the structures were developed and non-linear dynamic analyses were carried out to obtain a deep numerical insight into the seismic response of the three palaces, identifying the most vulnerable elements for each structure. The comparison between the numerical results and the damage survey showed that the numerical approach used in this study may be an adequate tool to properly evaluate the seismic response of historical masonry buildings. A comparative assessment of the results obtained for the different palaces was performed in terms of predicted damage distributions, energy density dissipated by tensile damage and displacement demand for the different macro-elements.

Keywords: failure analysis of historical masonry palace; crack patterns under seismic loads; 3D FE model and non-linear dynamic analysis; damage distribution.

1. Introduction

Historical masonry constructions were not conceived to properly withstand horizontal loads and are highly vulnerable to seismic actions, as also demonstrated during recent earthquakes in Italy [1-5]. Their high seismic vulnerability can be attributed mainly to the very low tensile strength of masonry, very small capacity to dissipate energy, inadequate connections between structural elements, poor out-of-plane capacity, presence of flexible floors/roofs and deterioration of materials over time [6-7]. A reliable seismic performance assessment of historical masonry constructions represents a fundamental step for the adoption of appropriate strategies aimed at reducing their seismic vulnerability and preserving the cultural and artistic value of the built heritage: for such reasons, the seismic assessment of masonry monumental buildings is currently a topic of great interest [8-14]. Several approaches and analysis methods can be used to evaluate the structural behavior of masonry structures, comprising simplified procedures based on structural macro-elements, limit analysis, discrete element (DE) method and micro-modelling or macro-modelling based on the finite element (FE) method [15-24]. The differences among the various approaches are mainly related to assumptions about the material and structural behavior, input parameters, modelling effort and computational time required. For historical masonry constructions, reliable structural analyses are fundamental in order to identify the most probable collapse mechanisms and address specific and not invasive retrofitting interventions.

Limit analysis is a frequently applied strategy for structural analysis and strengthening of historical masonry buildings. This method can be carried out without excessive computational effort, but it requires previous knowledge of the possible collapse mechanisms and can be used mainly to examine the ultimate state condition. The choice of the most probable mechanisms depends on the experience of the practitioner and may not be simple when a large variety of mechanisms are possible in the structure. Simplified procedures for the seismic vulnerability assessment of masonry building aggregates, typically widespread in historical centers of many Italian towns, have been proposed and numerically calibrated with reference to some case studies at small and large scales [25-26]. Masonry structures can be represented by discrete element models as an assembly of blocks with suitable interface laws. It is worth mentioning that discrete element approaches may encounter difficulties related to the analysis of buildings of relevant size, leading to a huge computational demand.

The equivalent frame model, generally used in combination with non-linear static analyses, is widely diffused in the engineering practice to investigate the global structural performance of masonry buildings with a reasonable computational effort and a small amount of mechanical parameters that may be quite simply defined through the results of standard tests. The accuracy of this method, which introduces strong simplifications and unavoidable approximations of the actual behavior and geometry of the building, depends on the consistency between the simplified hypothesis adopted and the real structural behavior.

In the literature, there are several significant examples of applications of the non-linear finite element (FE) method to study the seismic response of historical masonry constructions [27-32]. Depending on the level of accuracy and the simplicity desired, different modeling strategies can be adopted, including the micro-modelling and the macro-modelling approaches. The micro-modelling approach describes the behavior of units, mortar and the unit-mortar interface: due to the high level of detail in this type of modeling, its application is generally limited for the detailed analysis of portion of masonry structures. Conversely, the macro-modelling approach treats masonry as a homogeneous continuum, without any distinction among masonry constituents, and can be also applied for the analysis of large structures. Non-linear static analysis, which is generally based on macro-modelling approach, is one of the commonly used tools for seismic assessment of masonry buildings: on the other hand, non-linear dynamic analysis provides the most accurate and reliable assessment of the structural seismic response of historical masonry constructions when the non-linear behavior of the masonry material is properly defined. This study aims at pointing out that the use of advanced numerical tools, based on a macro-modeling approach and non-linear three-dimensional (3D)

dynamic analyses, can provide a thorough understanding of the seismic behavior of historical masonry buildings, highlighting all possible (both local and global) failure mechanisms.
The seismic sequence that occurred in Emilia-Romagna region, Northern Italy, in May-June 2012, caused heavy damages, showing mainly the seismic vulnerability of historical masonry constructions. A comprehensive description of the major damages occurred in existing masonry buildings and churches can be found in [33-34]. Detailed field surveys of some churches damaged during the seismic sequence are reported also in [35-36] along with the main results obtained through simplified procedures and advanced numerical simulations: numerical results were compared with real damages and collapses observed during in-situ surveys. The 2012 Emilia earthquake, whose magnitude reached M_L=5.9 (May 20) and M_L=5.8 (May 29), hit also the southern part of the Lombardia region and considerable damages were observed on several historical constructions located in the city of Mantua, where Politecnico di Milano has a large campus. The major damages suffered by three monumental masonry churches located in Mantua and the results of advanced numerical investigations performed on detailed 3D finite element (FE) models are presented in [37]: numerical results were discussed with respect to the cracks patterns registered during in-situ surveys. In [38] a multi-disciplinary approach was adopted to assess the structural safety and the seismic vulnerability of an historical palace in Mantua.
The historical center of Mantua was declared an UNESCO World Heritage Site in 2007 and was chosen as Italian Culture Capital in 2016. The cultural value of Mantua is outstanding, with several buildings being unique important examples of Italian Renaissance architecture. This paper describes the damage occurred in some important historical palaces in Mantua during the 2012 Emilia earthquake and presents the results of an extensive numerical investigation carried out on detailed FE models. The three palaces under study have a significant historical and architectural value, thus being some of the most important and renowned civic structures in Mantua.
The multi-disciplinary approach adopted to assess the structural safety and the seismic vulnerability of the three palaces involved different activities: historical analysis, documentary research, visual inspection, geometrical and construction typology documentation, photographic collection of damage and cracks patterns, development of sophisticated FE models, advanced numerical analyses to simulate the seismic response of the structures and to predict the seismic performance and damage distribution for different levels of seismic actions. This paper summarizes mainly the information and the results provided by the execution of documentary research, visual inspection and advanced numerical simulations. In spite of the unquestionable importance of these case studies, until now the seismic performance of the three buildings have not been studied through advanced numerical simulations and one of the aims of this study is to give a valuable contribution to fill the gap of knowledge about these three buildings. The results of the seismic assessment methodology adopted in this study allow estimating the possible damage patterns in the palaces during seismic events with different intensity levels, showing the most probable failure mechanisms. Comparisons among the seismic responses of the three palaces are made in terms of the predicted damage distribution, energy density dissipated by tensile damage (EDDTD) and displacement demand for the different macro-elements composing the structures.

2. Description of the historical buildings under study

This section provides a short description of the main historical, geometrical and constructive features of the buildings under study. A general view of each historical masonry building is shown in Fig. 1.

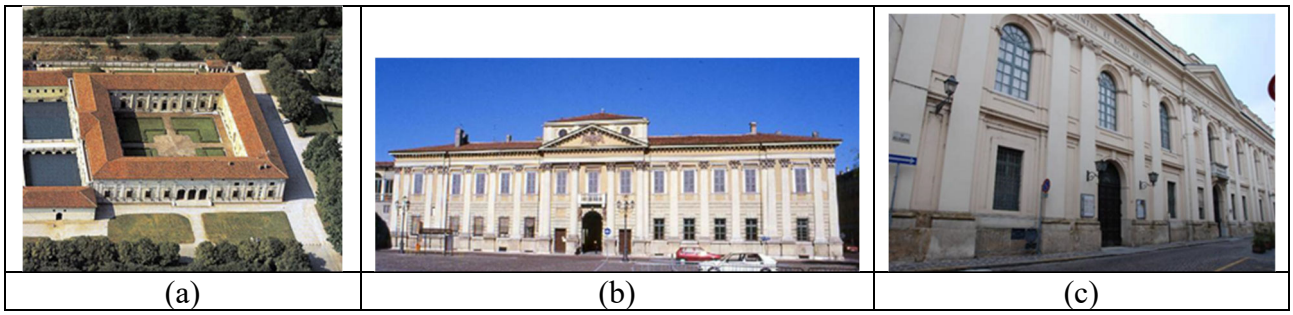

(a) (b) (c)

Fig. 1. General views of the historical masonry buildings under study. (a) Palazzo Te (1525-1535); (b) Palazzo d'Arco (1784); (c) Palazzo dell'Accademia (1773).

2.1. Palazzo Te

Palazzo Te is located in the suburbs (south part) of Mantua and is universally considered a masterpiece of the late Renaissance. It was built by Giulio Romano between 1525 and 1535, as a suburban residence for Federico II Gonzaga: the site chosen was that of the family's stables. The main block of Palazzo Te presents a large square plan with sides equal to about 70 m including a large inner courtyard, recalling an ancient Roman villa. The maximum height of the building is about 13 m in correspondence with the tympanum of the Loggia of David. The walls are about 11 m high and present an average thickness of about 65 cm: the openings are generally uniformly arranged. The north, east and west external sides present one or more arcades in the middle, while the south side is without entrance arcades and the arrangement of the windows does not follow a regular distribution, as observed for the other sides. The east side overlooking the large garden presents a high openings percentage due to the presence of large central arcades and a series of side Serlian windows. The sides delimiting the courtyard present a series of openings that are vertically and horizontally aligned. The east and west walls overlooking the courtyard are characterized by a series of niches that are 40 cm thick, both at the ground level and in correspondence with the mezzanines, and present a limited number of openings.

The bearing walls of the building are built in regular course bricks with lime mortar and plastered to simulate a coursed rubble. The covering elements are masonry (barrel, cloister and ribbed) vaults and wooden coffered slabs. The pitched roof consists of wooden truss beams and clay tiles.

Fig. 2 presents the plan and two sections of the building along with the main geometrical dimensions.

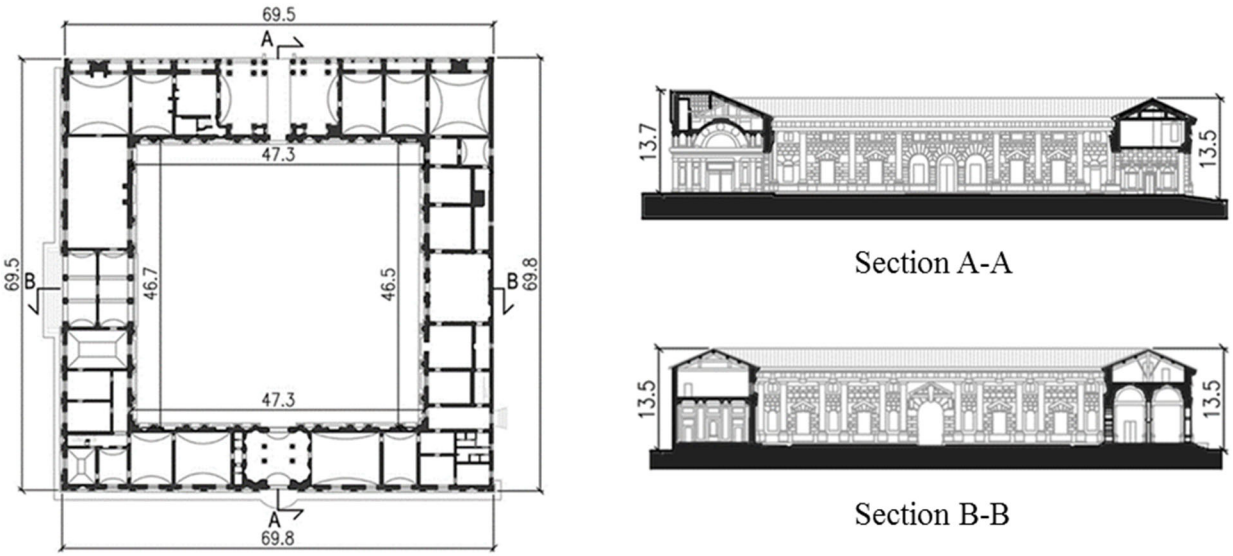

Fig. 2. Palazzo Te: plan, two sections and indication of the main geometrical dimensions.

2.2. Palazzo d'Arco

Palazzo d'Arco is the historical Mantuan residence of the ancient family of the Counts d'Arco: it is a wonderful example of neo-classical architecture in Mantua. The building, which arose on the ruins of an ancient medieval complex, was built by the neo-classical architect Antonio Colonna in 1784. During the Second World War the building was damaged by bombings and was restored between 1946-1960.

Currently, the complex consists of the main building overlooking Piazza d'Arco, the façade of which continues on the left with the building of the "Stables", which nowadays acts as a theatre. The long side is marked by pilasters and semicolumns supporting the tympanum that partially hides the square-plan block of the tall "Hall of Honour" rising above the remaining part of the building. Palazzo d'Arco presents a U-shaped plan with a courtyard that is closed by a large exedra. The south side exhibits a length equal to 46 m, while the north side presents a length equal to 38 m. The exedra, which is located along the entrance axis, connects the two wings of the building and presents a semicircular shape, except the two edges: it is 7.5 m high and is characterized by the presence of niches and large arches connecting the courtyard and the garden.

The complex exhibits three storeys (ground level, mezzanine and second level) and is composed of three wings rising uniformly up to 13 m, except the greenhouse, called "giardino d'inverno", that is 6.4 m high. On the left side, the adjacent theatre is 11 m high with plan dimensions of about 19 m x 24 m. The greenhouse is about 16.5 m long and is not aligned with the south wing of the building, protruding from one side. The long front side overlooking Piazza d'Arco, which is characterized by the central square block that is 17 m high, exhibits two rows of openings that are uniformly arranged: a similar regular arrangement of openings can be observed on the other sides.

The walls of the building are made of brick masonry and lime mortar, the coverings consist of masonry vaults and wooden slabs. The pitched roof is composed of wooden truss beams and clay tiles. Fig. 3 presents the plan and a section of the building along with the main geometrical dimensions.

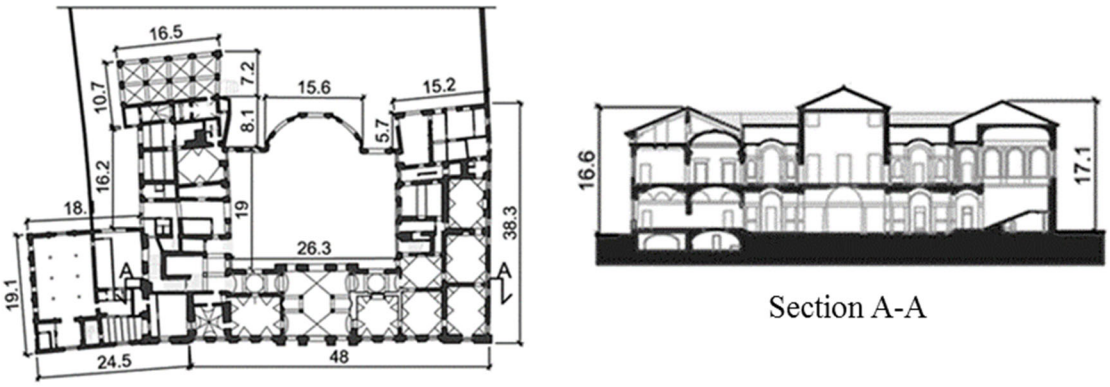

Fig. 3. Palazzo d'Arco: plan, section and indication of the main geometrical dimensions.

2.3. Palazzo dell'Accademia

Palazzo dell'Accademia, which is located in the north-east part of Mantua, rises on the ruins of an ancient medieval building renovated in the late fifteenth century. In 1773 the actual building was built on the project by Giuseppe Piermarini and under the direction of the architect Paolo Pozzo.

The building occupies an entire block along with the adjacent theatre and is characterized by a rectangular plan with an internal courtyard. The two long sides (east and west sides) present a length of about 51 m and 55 m, respectively, while the short sides (north and south sides) are about 34 m long: the short sides are not orthogonal with respect to the long sides. The height of the walls of the complex is 13.6 m, except the north and east sides that are about 16 m high due to the presence of a "veletta" in the upper part. The four walls overlooking the internal courtyard are 13.6 m high, except

the west wall that is 10.6 m high. The perimeter walls of the complex are characterized by several large openings that are horizontally and vertically aligned. In particular, the west and east walls overlooking the internal courtyard present large arcades and windows, both at the ground level and in the upper part.
The bearing walls of the building consist of brick masonry and lime mortar. The coverings are composed of masonry or wattle vaults and wooden or concrete-masonry slabs. The pitched roof consists of wooden truss beams and clay tiles.
Fig. 4 presents the plan and two sections of the building along with the main geometrical dimensions.

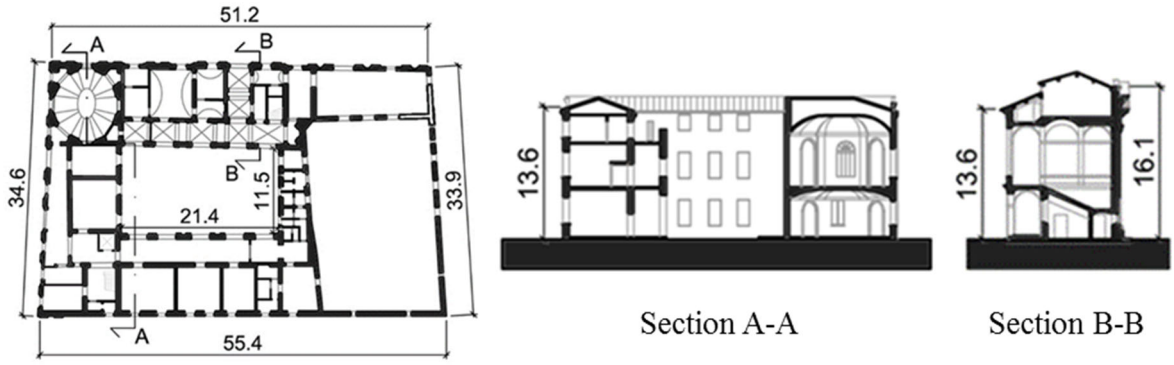

Fig. 4. Palazzo dell'Accademia: plan, two sections and indication of the main geometrical dimensions.

3. Damage survey

Extensive surveys of the cracks patterns of the three buildings were carried out after the 2012 Emilia earthquake: a photographic documentation of the main cracks is reported for each building in this section. It is worth mentioning that the majority of the cracks were due to the recent seismic sequence: in addition, some pre-existing cracks were enlarged by the seismic events.

3.1. Palazzo Te

The major damage is concentrated mainly in the north and east sides of the complex, while the south and west sides present negligible damage. Through-cracks have been observed in correspondence with the masonry walls and vaults, with consequent severe damage to the decorations and detachments of stucco fragments. The cracks surveyed were caused by the seismic sequence, taking into account the re-opening and consequent enlargement of some pre-existing cracks.

In detail, the main damage involves the following parts of the building, Fig. 5.

- "Room of the Sun and the Moon" (photos 1-3). A severe crack has been observed above and on the right of the door facing the "Loggia of the Muses" and the pre-existing crack on the wall in the north-east corner was enlarged. The stucco cornice and the plaster of the walls exhibit significant damage.
- "Loggia of the Muses" (photo 4). Marked cracks have been detected in correspondence with the short sides of the Loggia, where there are the doors connecting the Loggia and the "Room of the Sun and the Moon" on one side and the "Hall of the Horses" on the other side. Diagonal cracks have been observed in the upper part of the west wall, involving a multiple leaf wall and propagating on the frescoed lunette above the vault. Moreover, the earthquake has caused the fall of the stucco cornice decorating the lunette and fragments of the plaster along the crack involving the wall.
- "Hall of the Horses" and "Room of Eros and Psyche" (photos 5-7). A relevant crack has been surveyed in correspondence with the wall dividing the "Hall of the horses" and "Room of

Eros and Psyche", involving the whole corner. Moreover, the seismic event has caused the formation of new cracks along the stucco cornice of a window of the east wall of the "Room of Eros and Psyche".

- "Loggia of David", (photo 8). An evident crack has been observed along the south wall of the Loggia, in correspondence with the stucco cornice and the clay bas-relief above the door leading to the "Room of the Stuccoes", with a consequent fall of small stucco fragments. Moreover, many small cracks have been registered above the south door.
- "Room of the Emperors", (photo 9). A marked crack is visible along the wall separating the "Room of the Emperors" and the "Room of the Giants", with a consequent detachment of the plaster finish in the "Room of the Emperors".

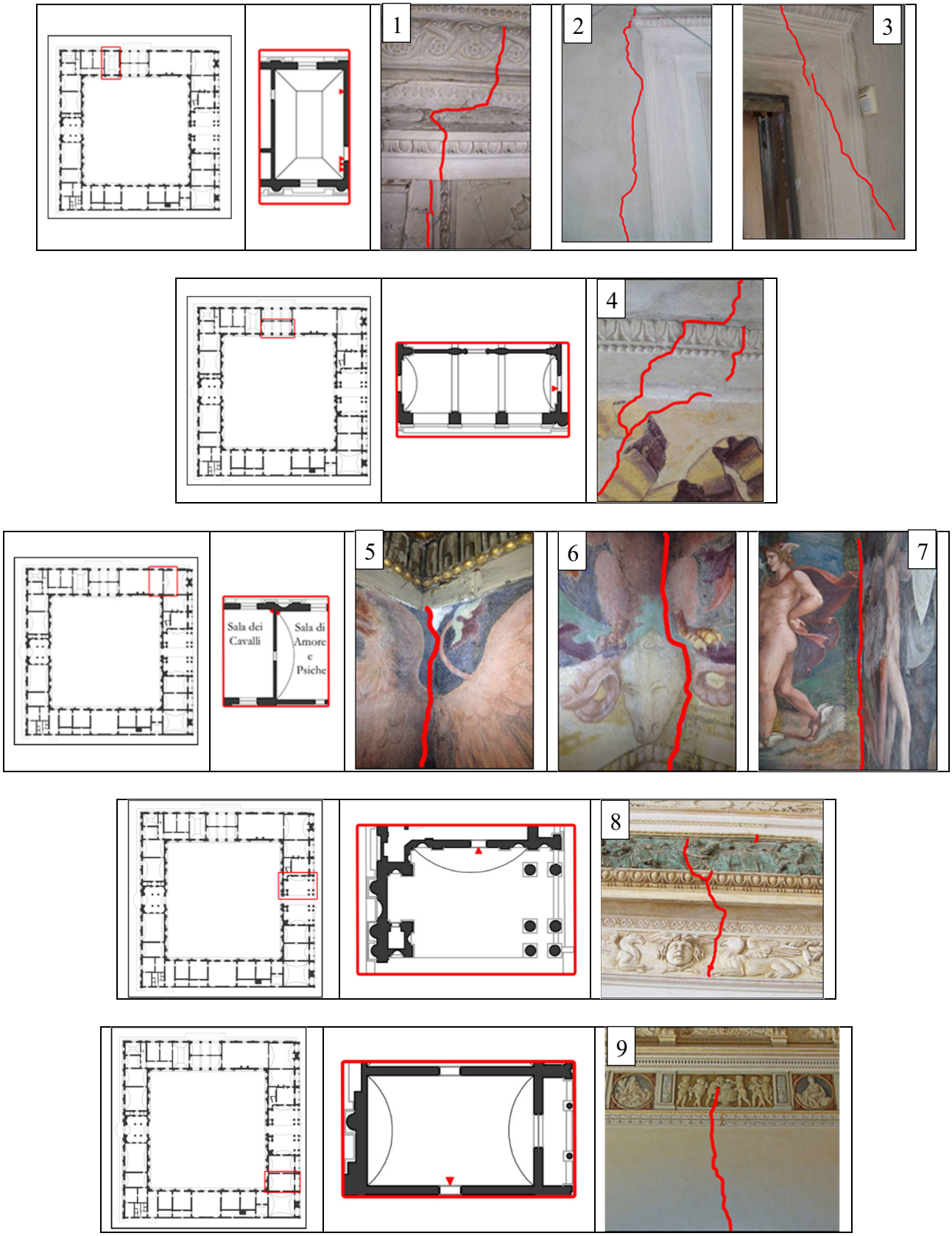

Fig. 5. Palazzo Te: photographic documentation of the crack patterns. 1. Room of the Sun and the Moon, ground floor, cornice. 2-3. Room of the Sun and the Moon, ground floor, wall. 4. Loggia of the Muses, ground floor, wall. 5-7. Hall of the Horses and Room of Eros and Psyche, ground floor, wall. 8. Loggia of David, ground floor, cornice and bas-relief above the door. 9. Room of the Emperors, ground floor, wall.

3.2. Palazzo d'Arco

The major damage is concentrated mainly in the greenhouse (orangerie) with prominent cracks along the connection regions between the cross vaults and the perimeter walls. Further evident cracks have been observed along the masonry vaults of the inner spaces and in some parts of the south-west façade of the building.

In detail, the main damage involves the following parts of the building, Fig. 6.

- Vaults of the greenhouse, (photos 1-6). Severe cracks, mainly due to the lack of adequate interlocking between masonry cross vaults and masonry walls, have been observed.
- South-west wall of the greenhouse, (photos 7-8). Marked cracks have been detected in correspondence with the corner wall, near the opening of the upper storey and along the wall connecting the greenhouse and the south-west wing of the building.
- Ceiling of the "Green Room", (photos 9-10). The seismic event has caused the formation of evident cracks in the wooden ceiling and in correspondence with the decorative elements; moreover, some pre-existing cracks have been furtherly enlarged. Notable cracks have been observed in the lintel of the door.
- Vaults of the corridor, (photo 11). Slight cracks have been detected in the masonry vaults of the first storey corridor leading to the "Hall of Ancestors" on one side and to the library on the other side. The major crack starts from the barrel vault, involving the arcade, and propagates along the ribbed vault.
- Vault of the library, (photo 12). Widespread cracks have been observed in correspondence with the barrel vault of the library, with a consequent progressive enlargement of the pre-existing cracks patterns.

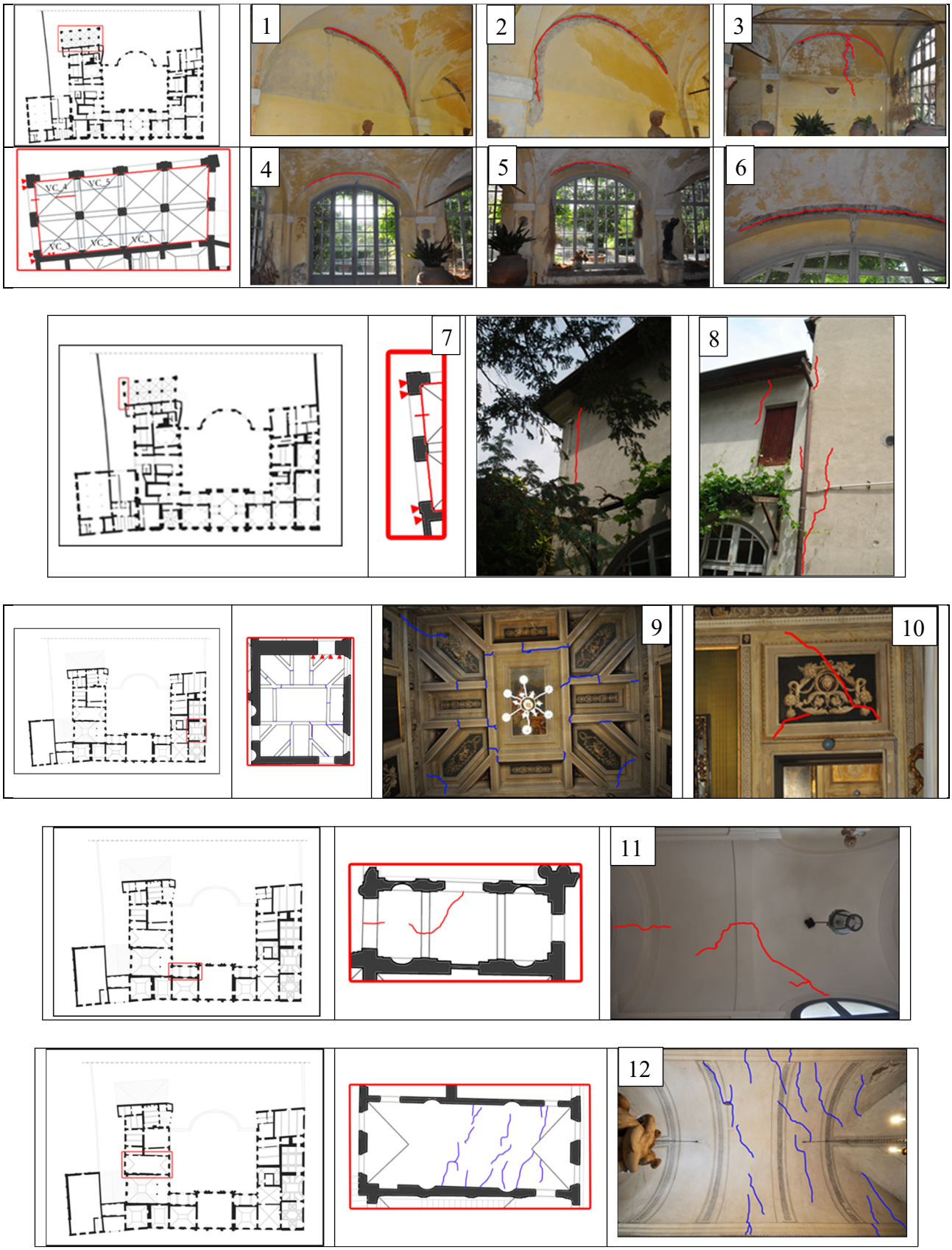

Fig. 6. Palazzo d'Arco: photographic documentation of the crack patterns. 1-6. Vaults of the greenhouse, ground floor. 7-8. South-west wall of the greenhouse, external wall. 9-10. Wooden ceiling and lintel of the door, Green Room, first floor. 11. Vaults of the corridor, first floor. 12. Vault of the library, first floor.

3.3. Palazzo dell'Accademia

The major damage is concentrated mainly in masonry arches and vaults with the formation of severe cracks patterns and consequent detachment and fall of rubble: it can be noted that also the wattle vaults have presented extensive damage. Further cracks have been registered in the lintels of doors and windows, as well as along the corners of masonry walls. No remarkable damage has been registered along the external and internal façades, except in some limited portions.

In detail, the main damage involves the following parts of the building, Fig. 7.

- Wall of the director's office, (photo 1). Vertical and horizontal through-cracks have been observed in correspondence with the door.
- Wall of the hallway, (photo 2). Vertical cracks have been detected in correspondence with the opening of the wall of the hallway, similarly to the cracks registered along the wall of the office of the director.
- Vault and wall of the "Staircase of Honour", (photo 3). Severe cracks have been observed in correspondence with the cross vault and the wall of the "Staircase of Honour" adjacent to the library.
- Wall of the corridor of the "Entrance of Honour", (photo 4). Severe cracks have been surveyed on the vertical structures delimiting the corridor adjacent to the entrance "Staircase of Honour".
- Vaults of the corridor of the "Entrance of Honour" (photos 5-10). Severe cracks and fall of materials have been observed in the corridor adjacent to the entrance "Staircase of Honour", in correspondence with the cross vaults and the arches between the vaults.
- Vaults of the "Oval Room", (photo 11). The pre-existing cracks of the wattle vaults have been enlarged by the seismic event.
- Vault of the library, (photo 12). Several cracks due to causes similar to those registered in the "Oval Room" have been registered in the wattle vault.
- Lintel of the door of the historical archive, (photo 13). A marked crack has been observed in the lintel of the door, with severe damage near the left support; moreover, a through-crack is visible along the upper right side.
- Wall of the stair, (photo 14). A severe crack is located in the corner of the wall of the stair leading to the second floor. The crack is almost vertical and propagates along the entire wall.

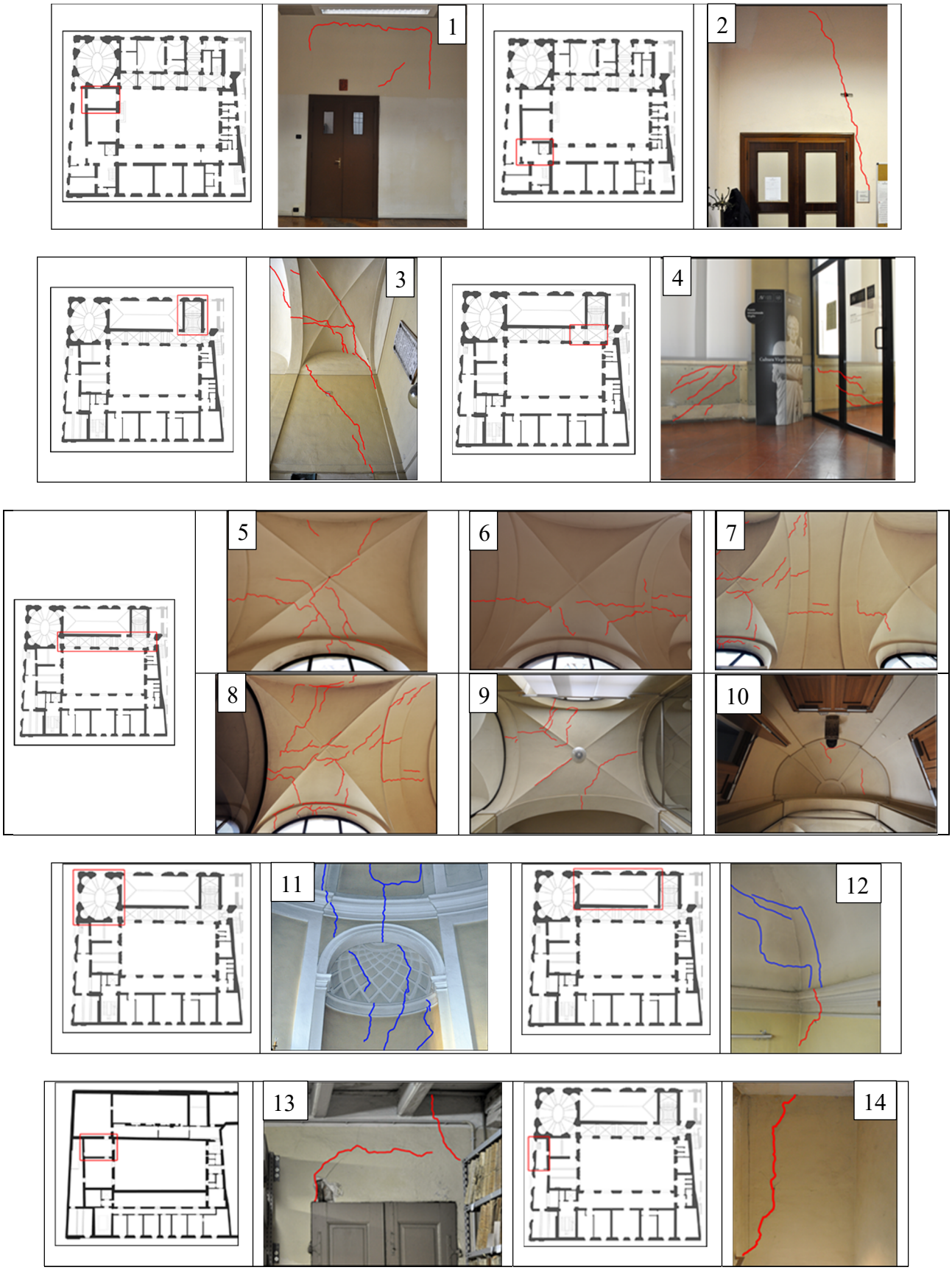

Fig. 7. Palazzo dell'Accademia: photographic documentation of the crack patterns. 1. Wall of the director's office, ground floor. 2. Wall of the hallway, first floor. 3. Vault and wall of the Staircase of Honour, ground floor-first floor. 4. Wall of the corridor/Entrance of Honour, first floor. 5-10. Vaults of the corridor/Entrance of Honour, first floor. 11. Vaults of the Oval Room, first floor. 12. Vault of the library, first floor. 13. Lintel of the door of the historical archive, second floor. 14. Wall of the stair, first and second floor.

4. FE models and material model adopted

Detailed three-dimensional FE models of the buildings under study were created through the software code Abaqus [39] using the drawings and the data collected from existing available documentations and during the survey phase. Figs. 8,10,12 show the geometrical and FE models of the three buildings. It is worth mentioning that the wooden structures of the coverings were not considered in the FE models. Four-node tetrahedral elements (about 430000 for Palazzo Te, 370000 for Palazzo d'Arco and 390000 for Palazzo dell'Accademia) having a size ranging between 20 cm and 40 cm were used in the discretization of the models. In each FE model, the most relevant macro-elements, indicated in Figs. 9,11,13 have been highlighted and investigated in detail in the following sections.

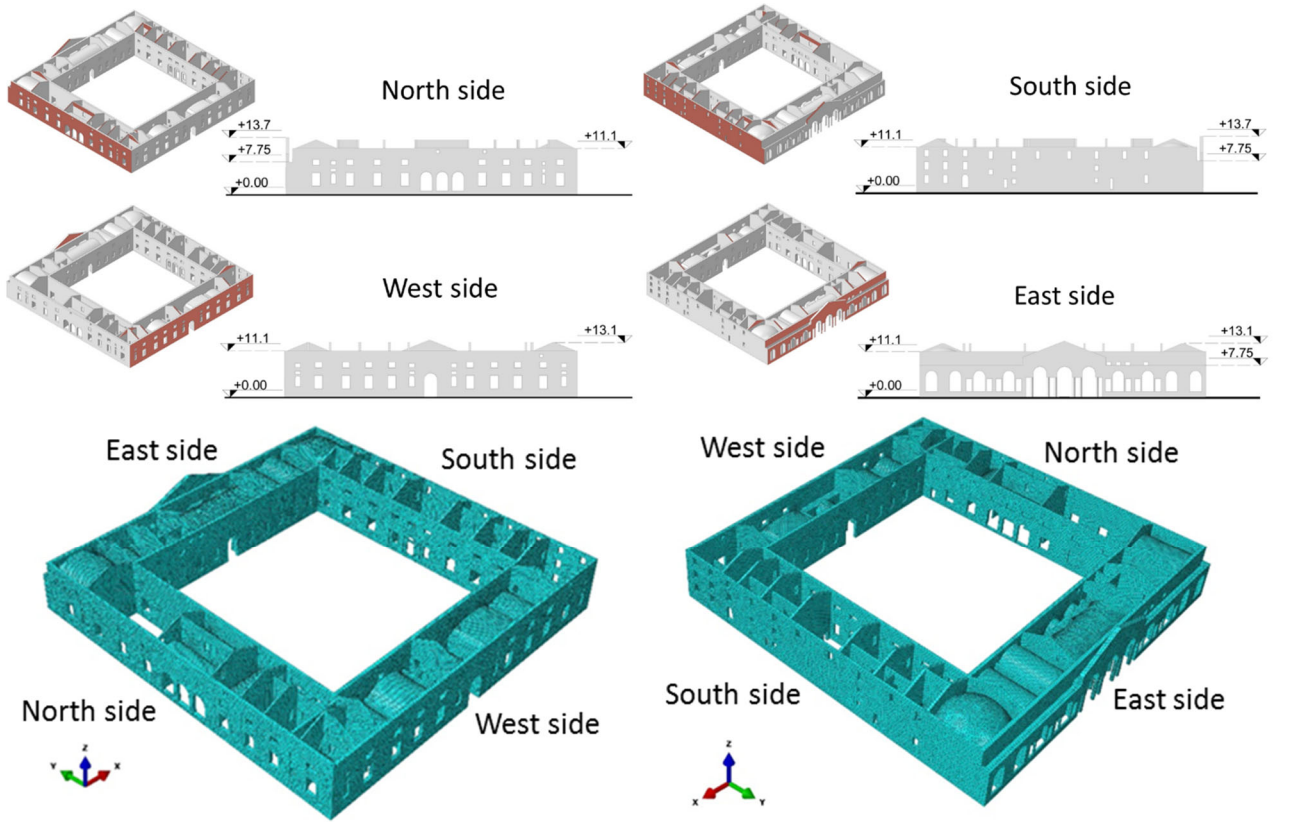

Fig. 8. Palazzo Te. Geometrical and FE models.

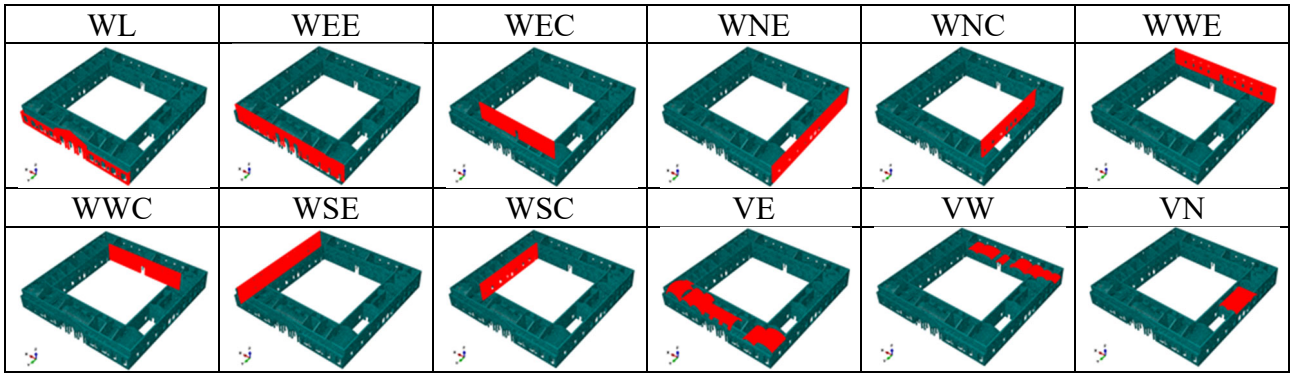

Fig. 9. Palazzo Te. Indication of the different macro-elements in the FE model.
Notation: WL=Loggia wall. WEE=External east wall. WEC=Courtyard east wall. WNE=External north wall. WNC=Courtyard north wall. WWE=External west wall. WWC=Courtyard west wall. WSE=External south wall. WSC=Courtyard south wall. VE=East vaults. VW=West vaults. VN=North vaults.

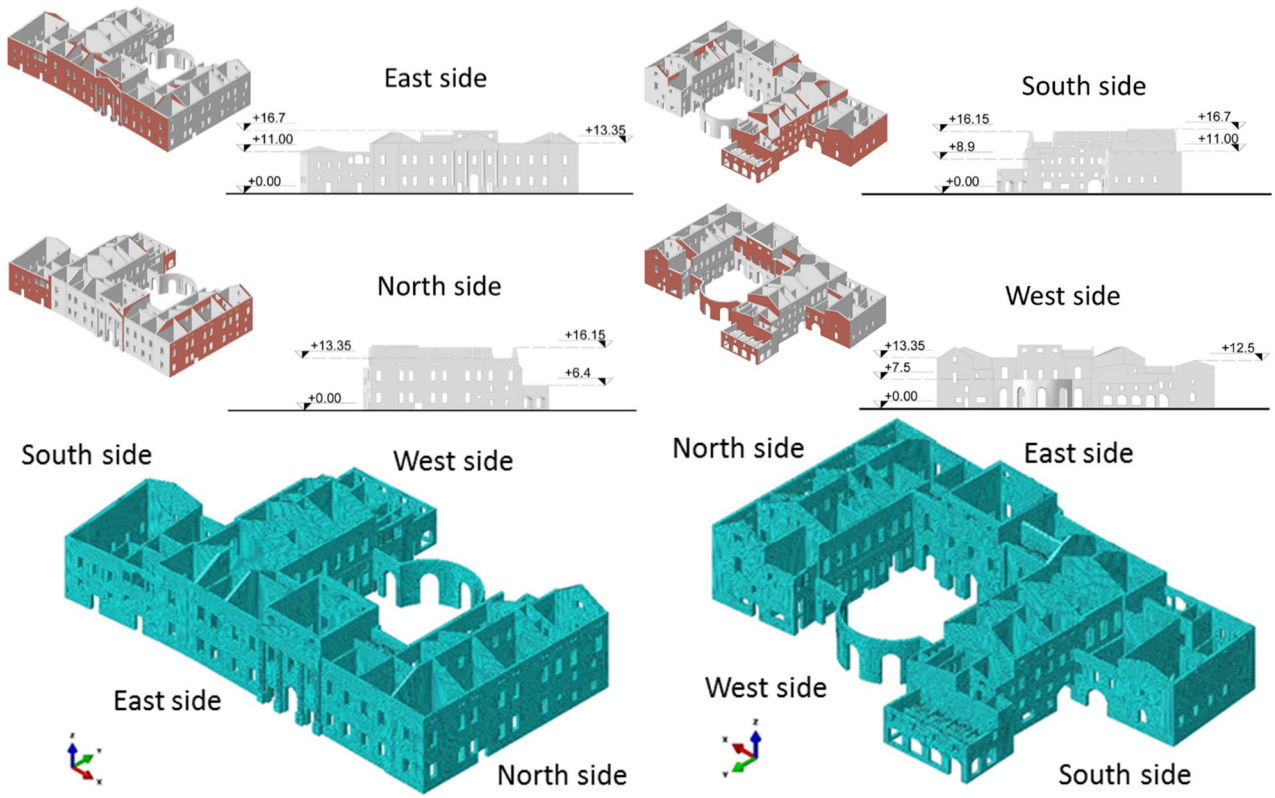

Fig. 10. Palazzo d'Arco. Geometrical and FE models.

CB	E	EEW	IEW	ENW	INW	NWW
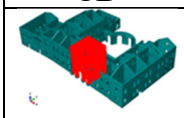	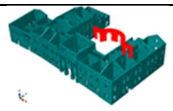	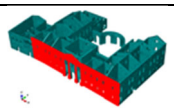	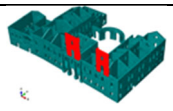	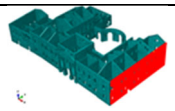	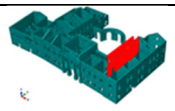	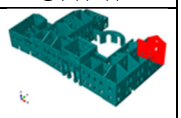
ESW	**ISW**	**SWW**	**OR**	**T**	**VI**	**VO**
	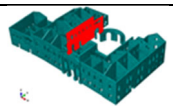	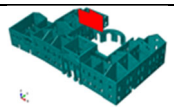	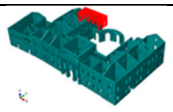	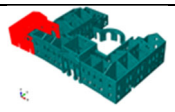	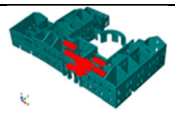	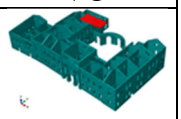

Fig. 11. Palazzo d'Arco. Indication of the different macro-elements in the FE model.
Notation: CB=Central block. E=Exedra. EEW=External East wall. IEW=Internal East wall. ENW=External north wall. INW=Internal north wall. NWW=North-west wall. ESW=External south wall. ISW=Internal south wall. SWW=South-west wall. OR=Orangerie. T=Theatre. VE=Entrance vaults. VS=Orangerie vaults.

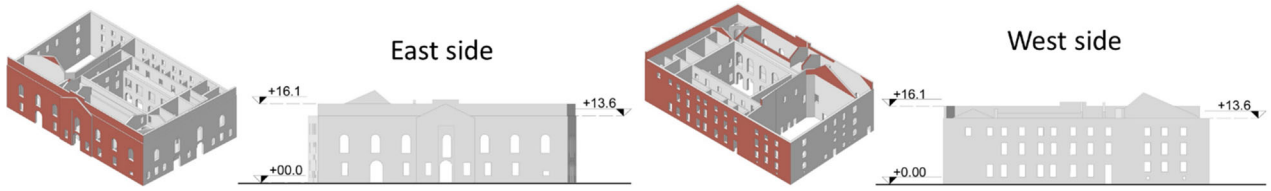

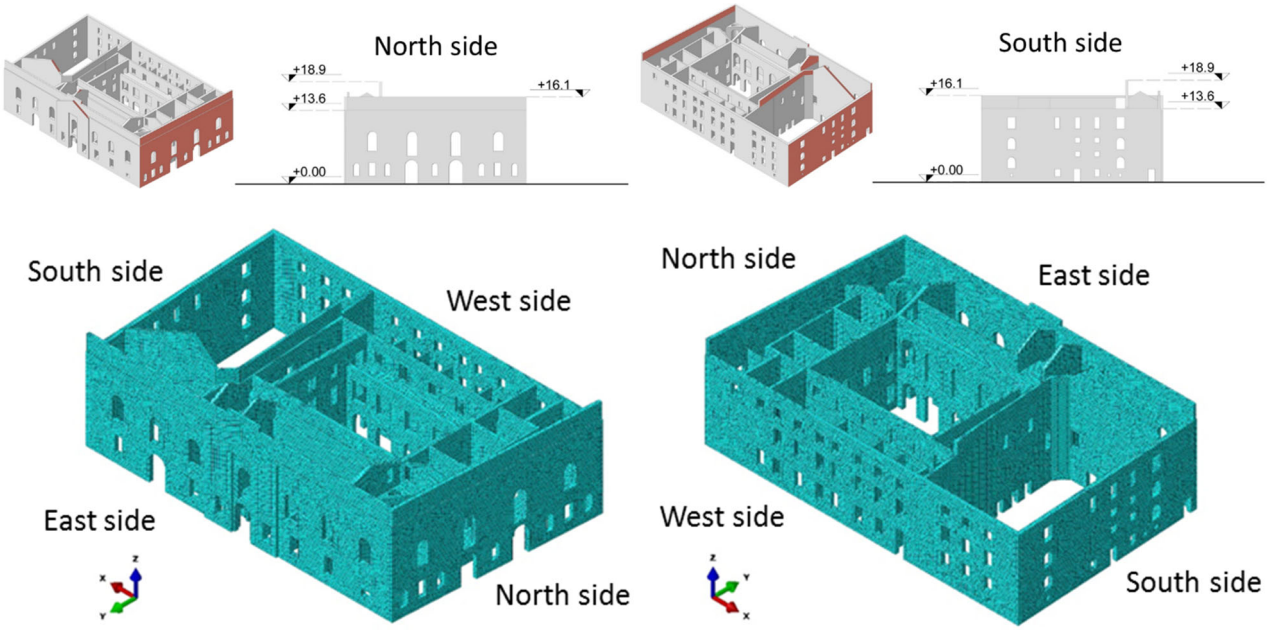

Fig. 12. Palazzo dell'Accademia. Geometrical and FE models.

EWC	NWC	WWC	SWC	TBW	EW	NW
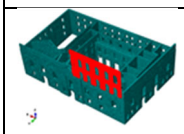	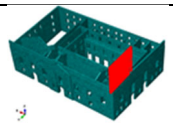	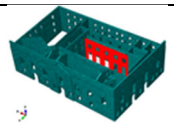	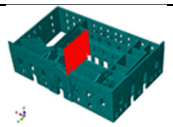	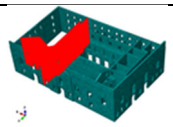	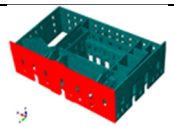	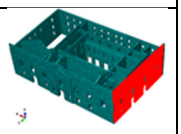
WW	**SW**	**VC1**	**VCG**	**VS**	**VB**	
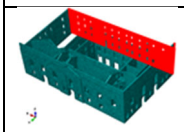	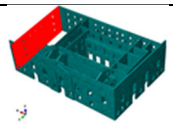	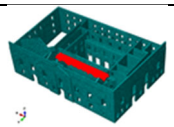	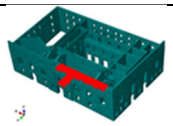	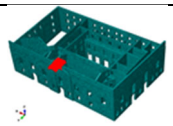	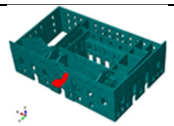	

Fig. 13. Palazzo dell'Accademia. Indication of the different macro-elements in the FE model.
Notation: EWC=Courtyard east wall. NWC=Courtyard north wall. WWC=Courtyard west wall. SWC=Courtyard south wall. TBW=Wall separating theatre and building. EW=East wall. NW=North wall. WW=West wall. SW=South wall. VC1=Corridor vaults, first floor. VCG=Corridor vaults, ground floor. VS=Vaults of the staircase. VB=Vaults of the basement.

The Concrete Damage Plasticity (CDP) model has been adopted to simulate the non-linear behavior of masonry. Although originally developed to describe the non-linear behavior of concrete [40-41], the utilization of such a model for masonry is commonly accepted in the literature after an appropriate adaptation of the main parameters. The CDP model is a continuum plasticity-based damage model that allows for different tensile and compressive strength, as the case of masonry, with distinct damage parameters in tension and compression.
The model assumes that the uniaxial tensile and compressive response is characterized by damaged plasticity, see Fig. 14.
Under uniaxial tension the stress-strain response follows a linear elastic relationship until the value of the failure stress σ_{to} is reached. The failure stress corresponds to the onset of micro-cracking in the material. Beyond the failure stress the formation of micro-cracks is represented macroscopically with a softening stress-strain response.
Under uniaxial compression the response is linear until the value of the initial yield σ_{co}. In the plastic range the response is typically characterized by stress hardening followed by strain softening beyond

the ultimate stress σ_{cu}. Such a representation, although somewhat simplified, captures the main features of the response of masonry.

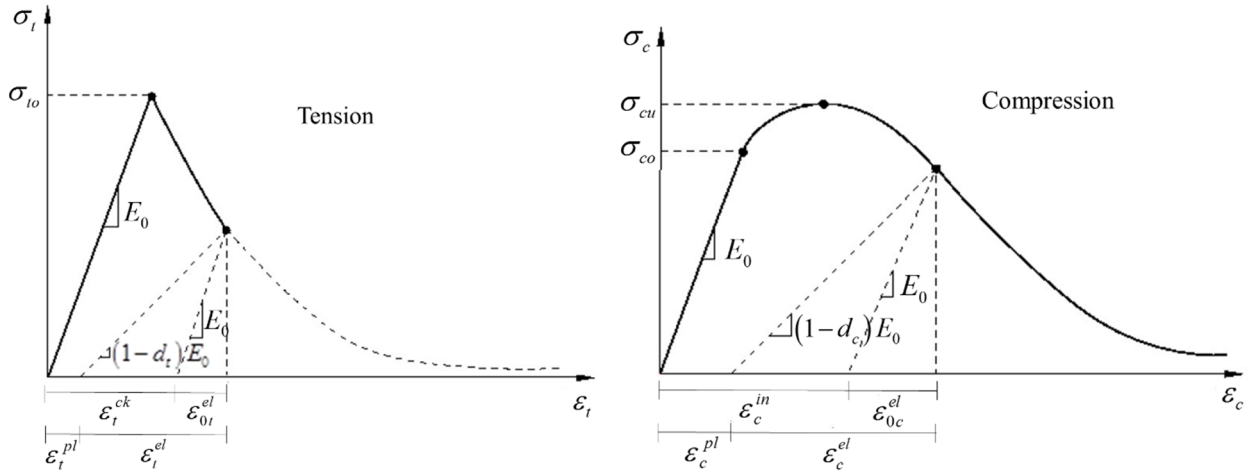

Fig. 14. Representation of the masonry constitutive behavior in tension and compression.

When the material is unloaded from any point on the strain softening branch of the stress-strain curve, the unloading response is characterized by a reduced elastic stiffness. The degradation of the elastic stiffness is different in tension and compression; in both cases, the effect is more pronounced as the plastic strain increases. The degradation of the elastic stiffness is characterized by two damage variables, denoted as d_t and d_c in tension and compression, respectively, which are increasing functions of the equivalent plastic strains: their values range between zero and one, representing a zero-damage state and complete damage state.
The following standard relationships define the uniaxial tensile σ_t and compressive σ_c stresses:

$$\sigma_t = (1-d_t)E_0(\varepsilon_t - \varepsilon_t^{pl}) \qquad (1)$$
$$\sigma_c = (1-d_c)E_0(\varepsilon_c - \varepsilon_c^{pl})$$

where E_0 is the initial elastic modulus, d_t and d_c are the scalar damage variables in tension and in compression, ε_t and ε_c are the total strain in tension and in compression, ε_t^{pl} and ε_c^{pl} are the equivalent plastic strain in tension and in compression.

The CDP model describes the post-failure behavior in tension as a function of the cracking strain ε_t^{ck}, which can be expressed as follows:

$$\varepsilon_t^{ck} = \varepsilon_t - \varepsilon_{0t}^{el} \qquad (2)$$

where ε_t is the total tensile strain and $\varepsilon_{0t}^{el} = \frac{\sigma_t}{E_0}$ is the elastic tensile strain.

The tensile equivalent plastic strains ε_t^{pl} can be obtained as follows:

$$\varepsilon_t^{pl} = \varepsilon_t^{ck} - \frac{d_t}{(1-d_t)}\frac{\sigma_t}{E_0} \qquad (3)$$

Similarly, the post-failure behavior in compression is related to the inelastic strain ε_c^{in}, which can be expressed as follows:

$$\varepsilon_c^{in} = \varepsilon_c - \varepsilon_{0c}^{el} \qquad (4)$$

where ε_c is the total compressive strain and $\varepsilon_{0c}^{el} = \frac{\sigma_c}{E_0}$ is the elastic compressive strain.

The compressive equivalent plastic strain ε_c^{pl} can be evaluated from Eq. (5):

$$\varepsilon_c^{pl} = \varepsilon_c^{in} - \frac{d_c}{(1-d_c)}\frac{\sigma_c}{E_0} \tag{5}$$

In addition, the CDP model takes into account the effect of closing of previously formed cracks under cyclic loading conditions, which results in the recovery of the compression stiffness. In fact, experimental observations in most quasi-brittle materials indicate that the compressive stiffness is recovered upon crack closure as the load changes from tension to compression. On the other hand, the tensile stiffness is not recovered as the load changes from compression to tension once crushing microcracks have developed.
In uniaxial stress conditions the loss of elastic stiffness is computed as follows:

$$(1-d) = (1-s_t d_c)(1-s_c d_t) \tag{6}$$

where s_t and s_c are functions of the stress state and are introduced to model the stiffness recovery effects due to stress reversal. They are computed using the following equations:

$$\begin{cases} s_t = 1 - w_t H(\sigma_{11}) \\ s_c = 1 - w_c (1 - H(\sigma_{11})) \end{cases} \tag{7}$$

where w_t and w_c are the weight factors (assumed as material properties) that control the recovery of tensile and compressive stiffness upon load reversal: they can range from zero, which represents no stiffness recovery, to one, which represents a total stiffness recovery. $H(\sigma_{11})$ is the Heaviside function that is assumed equal to 1 if $\sigma_{11}>0$ and equal to 0 if $\sigma_{11}<0$. Fig. 15 illustrates a uniaxial load cycle assuming the default behavior adopted in Abaqus [39], which corresponds to $w_t = 0$ and $w_c = 1$.

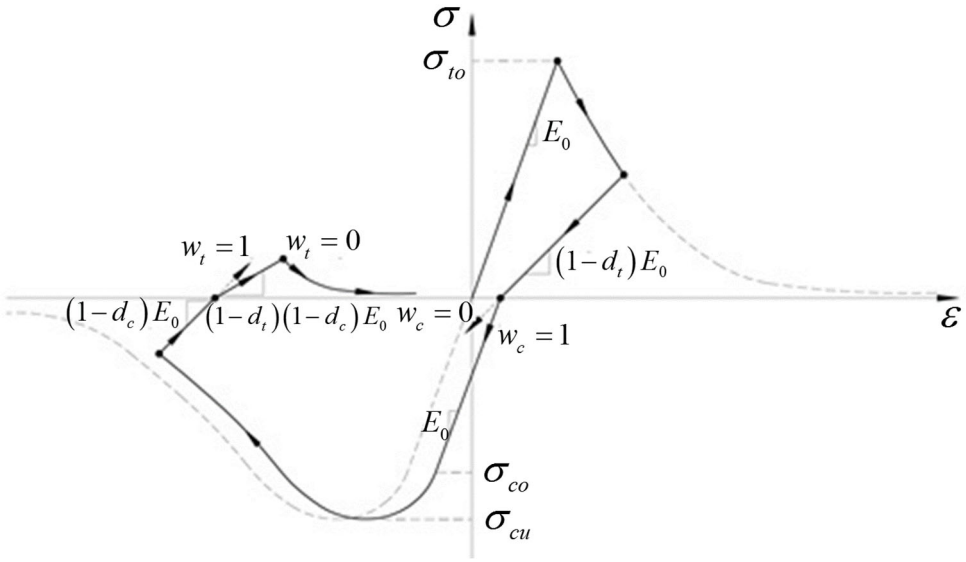

Fig. 15. Uniaxial load cycle (tension-compression-tension) assuming default values for the stiffness recovery factors: $w_t = 0$ and $w_c = 1$

The CDP model uses a Drucker-Prager strength criterion, modified through a parameter, K_c, which represents the ratio between the second stress invariant on the tensile meridian and the one on the compressive meridian, and assumes a non-associated potential flow rule. The value of K_c is set equal

to 0.666, as suggested by the Abaqus users guide [39]. A regularization of the tensile corner has been performed using a correction parameter, called eccentricity: such a parameter defines the rate at which the plastic flow potential approaches the asymptote, i.e. the flow potential tends to a straight line as the eccentricity tends to zero. A value equal to 0.1 is adopted for the eccentricity parameter. It is worth mentioning that smaller values of the eccentricity parameter may cause convergence problems when the material is subjected to low confining pressures because of the very tight curvature of the flow potential [39]. The dilatation angle ψ, which is the angle due to a variation in volume of the material following the application of a shear force, is set equal to 10°, in agreement with experimental evidences available in the literature [42]. The strength ratio f_{b0} / f_{c0}, which is the ratio of initial equibiaxial compressive yield stress to initial uniaxial compressive yield stress, is assumed equal to 1.16, as suggested in [43].

Material models exhibiting softening behavior and stiffness degradation may lead to severe convergence difficulties in implicit analysis programs, such as Abaqus/Standard. Some of these convergence difficulties can be overcome by using a viscoplastic regularization of the constitutive equations. The CDP model can be regularized using viscoplasticity with a small value for the viscosity parameter that usually helps improve the convergence rate of the model in the softening branch, without compromising results.

The visco-plastic strain rate component $\dot{\varepsilon}_v^{pl}$ and the viscous stiffness degradation variable d_v are expressed as:

$$\dot{\varepsilon}_v^{pl} = \frac{1}{\mu}(\varepsilon^{pl} - \varepsilon_v^{pl}) \qquad (8)$$

$$\dot{d}_v = \frac{1}{\mu}(d - d_v)$$

where μ is the viscosity parameter representing the relaxation time of the viscoplastic system, ε^{pl} is the plastic strain component and d is the degradation variable.

The stress–strain relationship of the viscoplastic model becomes as:

$$\sigma = (1 - d_v) E_0 (\varepsilon - \varepsilon_v^{pl}) \qquad (9)$$

If the viscosity parameter is different from zero, output results of the plastic strain and stiffness degradation refer to the viscoplastic values ε_v^{pl} and d_v. A value of the viscosity parameter equal to 0.002 has been assumed in this study.

In the absence of available results from experimental tests for the case studies, the mechanical parameters of the material are selected referring to Table C8A.2.1 in Circolare 02/2009 [45-46]. A masonry typology with quite regular texture constituted by clay bricks and lime mortar is considered. The parameters used in the non-linear dynamic analyses are the following: (1) the density and the elastic modulus are equal to 1800 kg/m^3 and 1500 MPa, respectively; (2) the compressive strength is equal to σ_{cu}=2.4 MPa. The tensile strength is set equal to σ_{to}=0.15 MPa, obtaining a ratio between the tensile and compressive strength equal to about 0.06. The scalar damage variable in tension (d_t), representative of the stiffness degradation of the material, is assumed to vary linearly: the value ranges from zero, for the strain corresponding to the stress peak, to 0.95, for the ultimate strain value of the softening branches. Table 1 specifies the uniaxial stress-strain values assumed in compression and in tension and the evolution of the scalar damage variable in tension.

Table 1. Uniaxial stress–strain values and scalar damage values utilized in the CDP model for masonry.

Compression		Tension		Damage in tension	
Stress [MPa]	Inelastic strain [-]	Stress [MPa]	Cracking strain [-]	d_t	Cracking strain [-]
1.9	0	0.150	0	0	0
2.4	0.0051	0.075	0.00025	0.95	0.00121
0.96	0.0102	0.018	0.00057		
0.48	0.0307	0.009	0.00121		

5. Numerical simulations

Eigen-frequency analyses were conducted on the 3D FE models in order to obtain a preliminary insight into the dynamic behavior of the buildings under study, identifying the main vibration modes, the corresponding periods and the participating mass ratios.
The seismic response of the three buildings was investigated through non-linear dynamic analyses using the real accelerograms registered on May 29 during the 2012 Emilia seismic sequence. The same accelerograms, presenting equal intensity in the two orthogonal directions, were used for the numerical simulations of all the buildings. Fig. 16 shows the two horizontal components of the accelerogram with PGA=0.15g applied in the X and Y directions and the corresponding acceleration response spectra. The duration of the acceleration time histories was assumed equal to 10 s because of the high computational demand required by the analyses.
Three different PGA values, ranging between 0.05g and 0.15g, were used in the non-linear dynamic analyses. The non-linear dynamic analyses with PGA=0.05g aim at simulating the seismic response of the buildings to earthquakes of small magnitudes and comparing the results with the real damage observed after the 2012 earthquake. The non-linear dynamic analyses with PGA=0.1g and PGA=0.15g provide useful information about the seismic response and damage distribution of the buildings for higher PGA values than those registered in Mantua during the 2012 Emilia earthquake.
The tensile damage contour plots obtained at the end of the numerical simulations are shown for each building; then, the energy density dissipated by tensile damage (EDDTD) and the maximum normalized displacements are reported for the main macro-elements of each building.
The main aims of the numerical simulations are: (i) to identify the most vulnerable elements for each building; (ii) to assess the damage evolution and the main response parameters variations for different levels of seismic action.

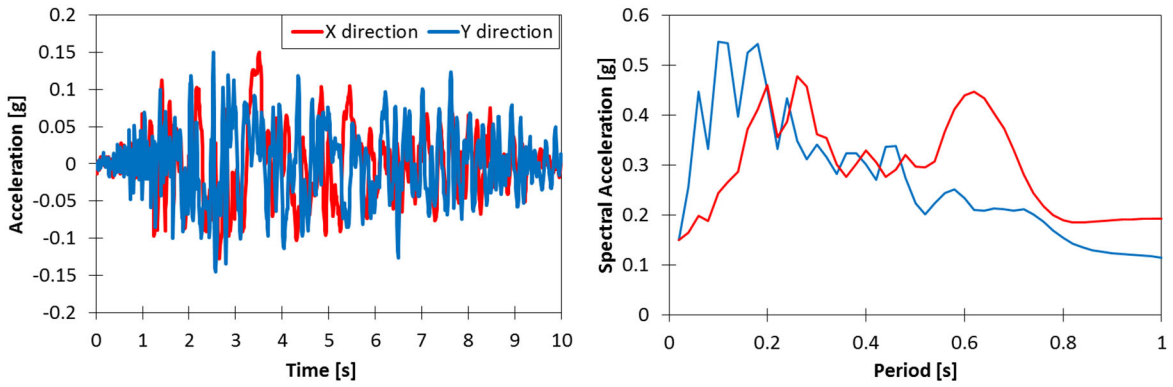

Fig. 16. Horizontal components of the accelerogram (Mirandola, 29 May 2012) used in the non-linear dynamic analyses: North-South (N-S) component (red) applied in the X direction, East-West (E-W) component (blue) applied in the Y direction.

5.1. Palazzo Te

Fig. 17 shows the deformed shapes and the corresponding periods of the main vibration modes with participating mass ratio (PMR) larger than about 5% for Palazzo Te: moreover, the distribution of the first three hundred modes in the two orthogonal directions is presented.
The first two main modes are Mode 3 (T=0.253 s), involving the upper part of the walls of the Loggia and the external east wall with PMR equal to 5.52% in the Y direction, and Mode 15 (T=0.153 s), involving the north wall with PMR equal to 7.6% in the X direction. It is interesting to observe that there is a large difference between the periods of the first two main modes. The most relevant modes are Mode 17 (T=0.148 s), involving the east and north sides with the largest PMR (14.6%) in the X direction, and Mode 25 (T=0.128 s), involving the north side with the largest PMR (15.3%) in the Y direction. The first three hundred modes correspond to a total PMR of 83% in the X direction and 82% in the Y direction.
It can be noted that the main vibration modes present a period corresponding to high amplifcations of the spectral accelerations, above all in the Y direction: the critical elements of the building result the east and north sides.

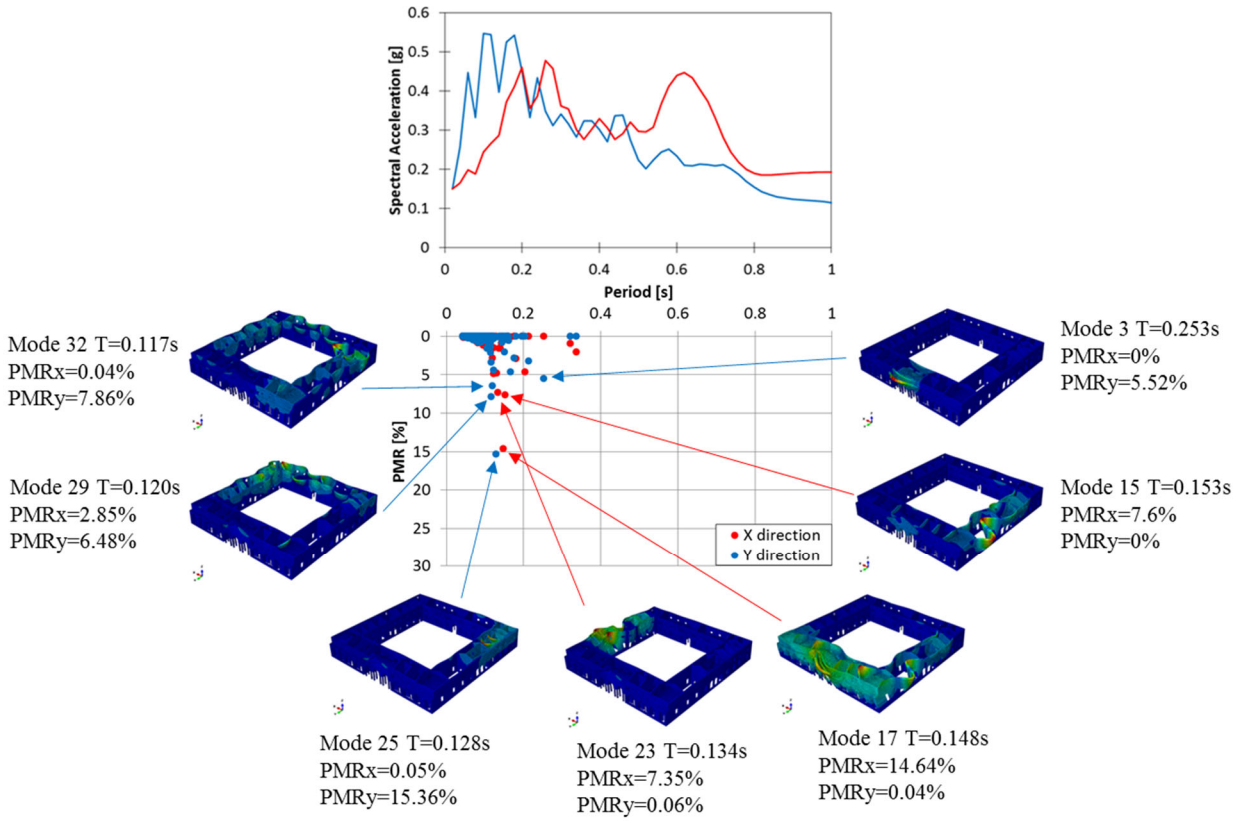

Fig. 17. Palazzo Te. Distribution of the first three hundred modes in the X and Y directions. Deformed shapes and corresponding periods of the main vibration modes with indication of the participating mass ratios in the X and Y directions.

Fig. 18 and Fig. 19 show the tensile damage contour plots of Palazzo Te at the end of the non-linear dynamic analyses with different PGA.
-The results of the non-linear dynamic analysis with PGA=0.05g show the onset of damage in the critical elements of the building. It can be noted that the vaults present an evident damage in the connection regions with the walls. A good correlation can be observed between the numerical results and the real damage observed after the 2012 earthquake: in fact, there is an onset of cracks along the corners of the walls, as registered in the “Hall of the Horses” and in the “Room of Eros and Psyche”: such cracks can be enlarged by the thrusts of the vaults on the walls.

-A moderate damage can be observed in different parts of the building at the end of the non-linear dynamic analysis with PGA=0.15g. An onset of damage is registered in correspondence with the corners of the walls. The damage is widespread not only in the external walls and in the walls overlooking the courtyard, but also in the orthogonal partition walls subdividing the internal spaces. The masonry vaults of the south, east and west sides present cracks in the connection regions with the perimeter walls: damage increases in correspondence with the vaults covering long spans, causing a stiffness reduction of such vaults.
-A significant increase of damage is observed in the case of non-linear dynamic analysis with PGA=0.25g. Damage is considerably widespread in the vaults and in the external and internal walls. The onset of damage visible in the external walls in the case of smaller PGA increases significantly. Horizontal cracks can be seen in the spandrels in correspondence with the openings: moreover, shear cracks can be observed along the piers (in-plane mechanism), then reducing their strength. The thrusts of the vaults on the walls enlarge the cracks, triggering possible overturning mechanisms. The partition walls and the vaults covering long spans exhibit widespread damage.

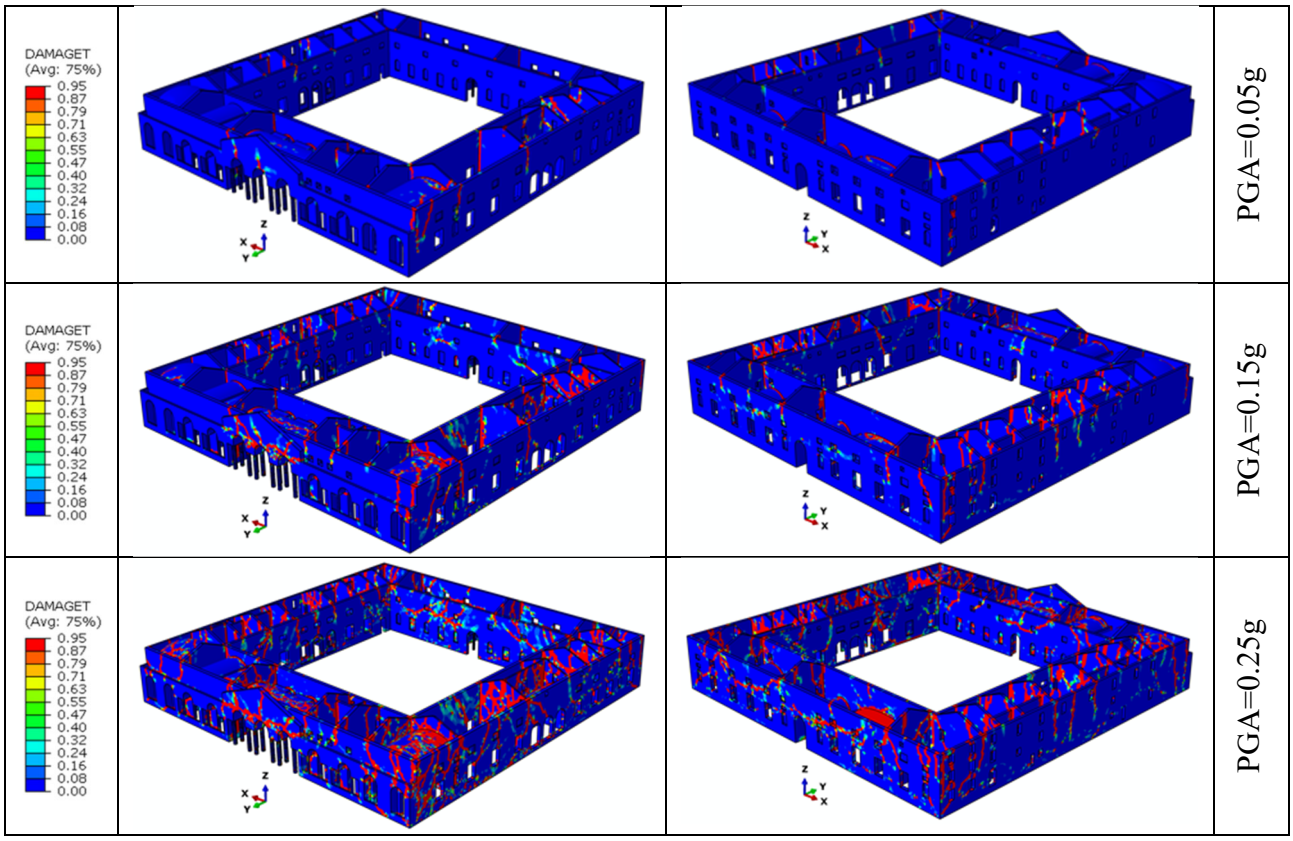

Fig. 18. Palazzo Te. Tensile damage contour plot at the end of the non-linear dynamic analyses with different PGA: axonometric views.

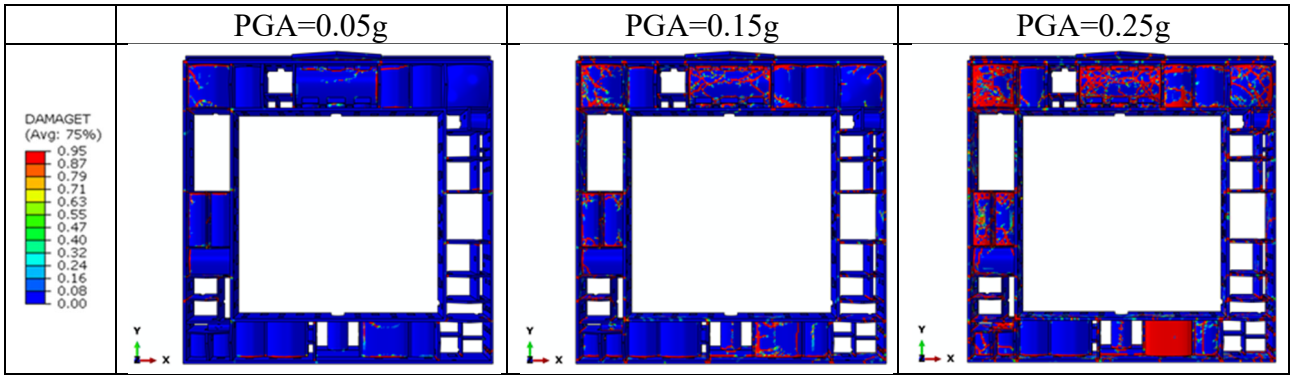

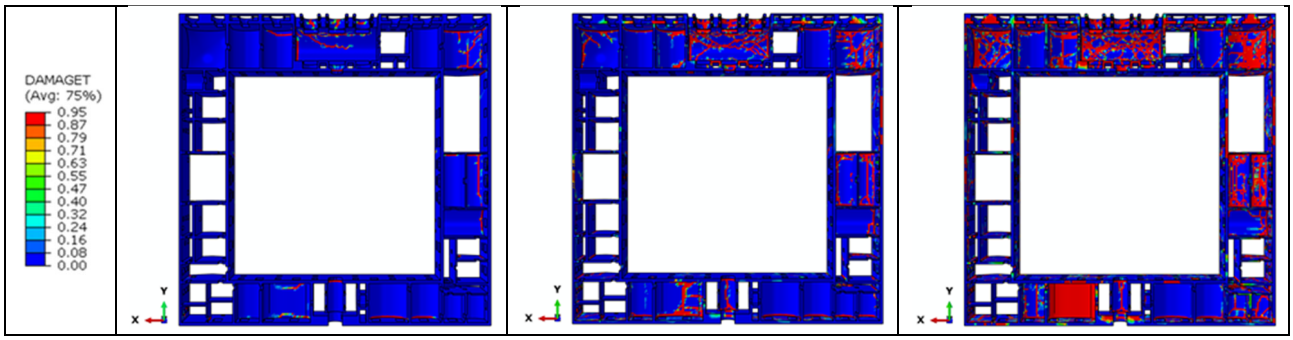

Fig. 19. Palazzo Te. Tensile damage contour plot at the end of the non-linear dynamic analyses with different PGA: top and bottom views.

Fig. 20 shows the energy density dissipated by tensile damage (EDDTD) for the main macro-elements of Palazzo Te at the end of the non-linear dynamic analyses with different PGA. It has to be pointed out that the vaults are the most damaged elements of the building. Under PGA=0.25g, the maximum value of EDDTD is registered for vault V7 in the west side and vault V17 in the north-east corner. High values are computed also for vaults V1 and V2 in the south side, vault V4 in the south-east corner, vaults V13, V15 and V16 in the north side.
As regards the transversal walls, the highest values of EDDTD are registered for walls T13-T17 in the north side, walls T4-T5 in the south side and T20 in the east side. Among the external and internal walls, the wall of the Loggia (WL) presents the highest EDDTD value.
It can be noted that there is a large increase of EDDTD for all the macro-elements in the case of PGA=0.25g.

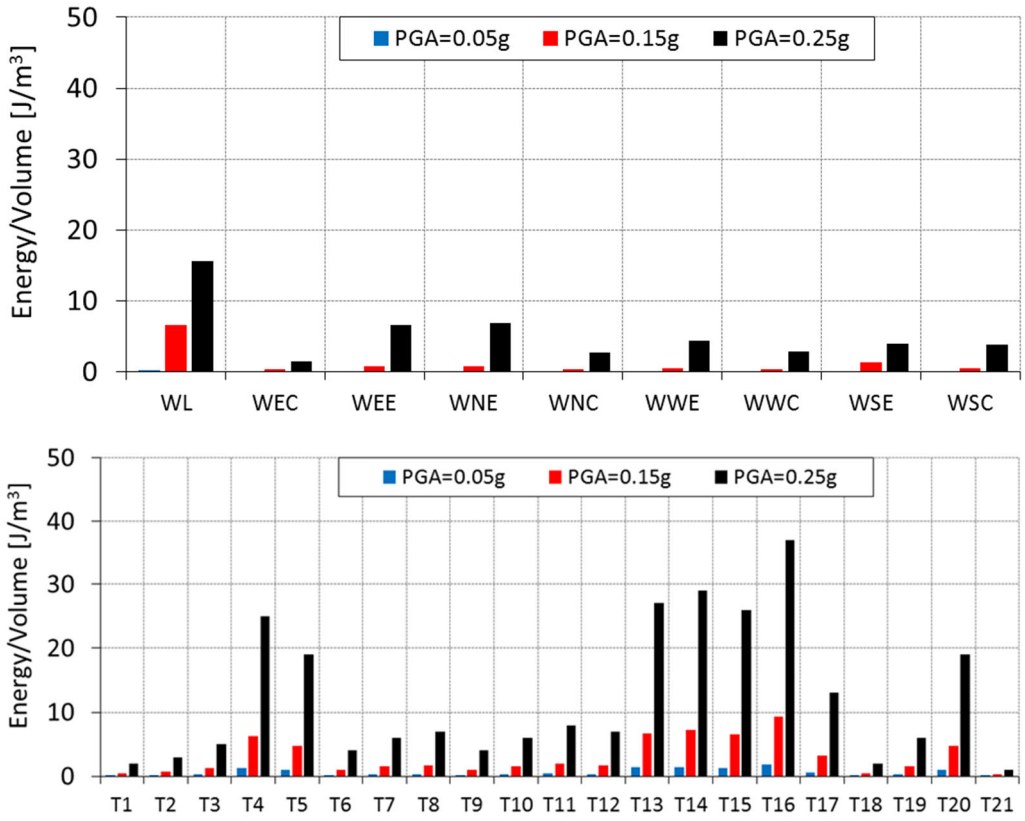

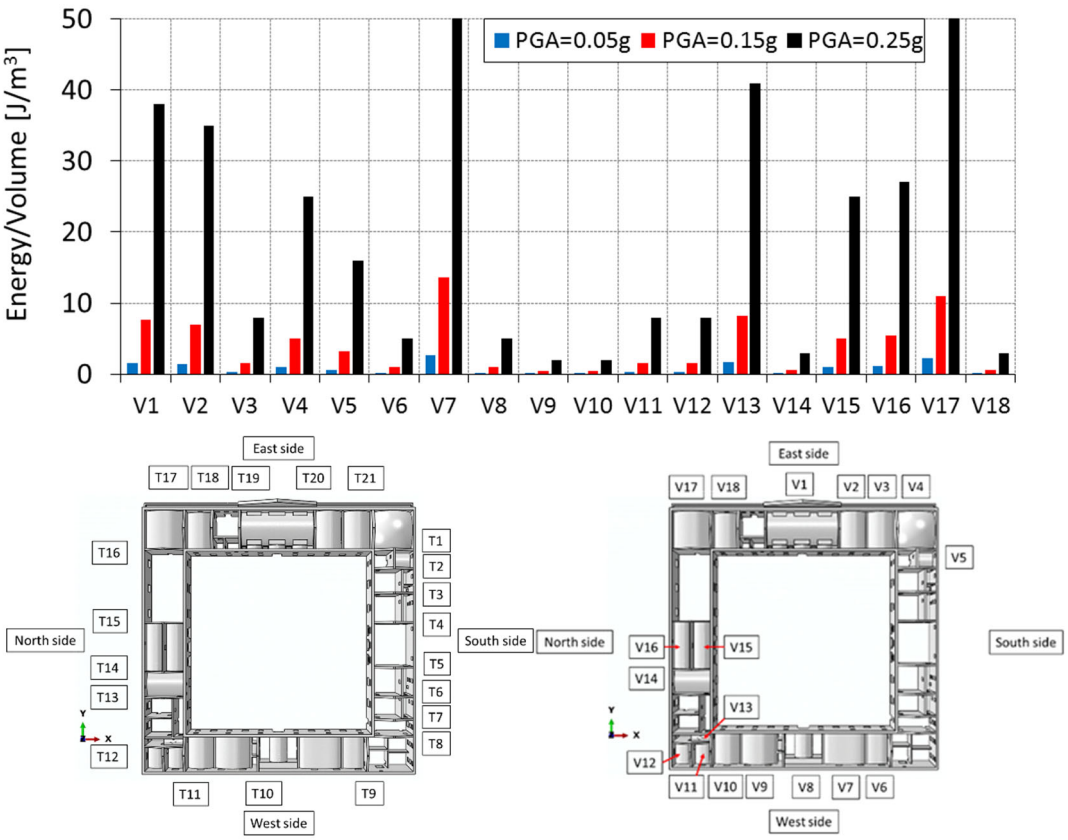

Fig. 20. Palazzo Te. Energy density dissipated by tensile damage (EDDTD) for the different macro-elements (walls, transversal walls, vaults) at the end of the non-linear dynamic analyses with different PGA.

Fig. 21 shows the maximum normalized displacements (top displacement/height) registered in the X and Y directions for the main macro-elements of Palazzo Te during the non-linear dynamic analyses with different PGA. The external north wall (WNE) presents the largest normalized displacement (larger than 2%) in the X direction: high values (larger than 1%) are registered also for the courtyard north wall (WNC), the external south wall (WSE) and the courtyard south wall (WSC). The wall of the Loggia (WL) presents the largest normalized displacement (larger than 2%) in the Y direction: high values (larger than 1.35%) are registered also for the external west wall (WWE) and the courtyard west wall (WWC).

As regards the transversal walls, the highest normalized displacements are registered for the walls T13-T16 (north side) and walls T4-T5 (south side) in the Y direction and walls T20-T17 (east side) in the X direction.

Fig. 22 shows the maximum vertical displacements registered for the main vaults during the non-linear dynamic analyses with different PGA. It is important to highlight that vaults V7 (west side), V1 (east side) and V17 (north-east corner) present considerable vertical displacements (larger than 20 cm), indicating an onset of a probable collapse.

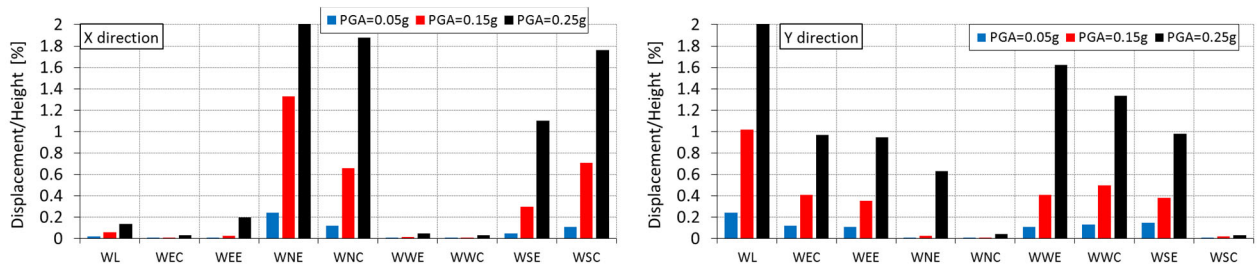

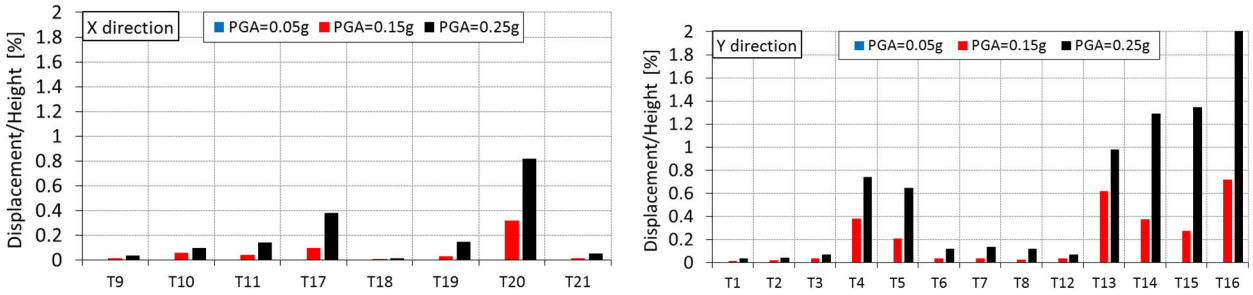

Fig. 21. Palazzo Te. Maximum normalized displacements (top displacement/height) registered for the main macro-elements in the X and Y directions during the non-linear dynamic analyses with different PGA.

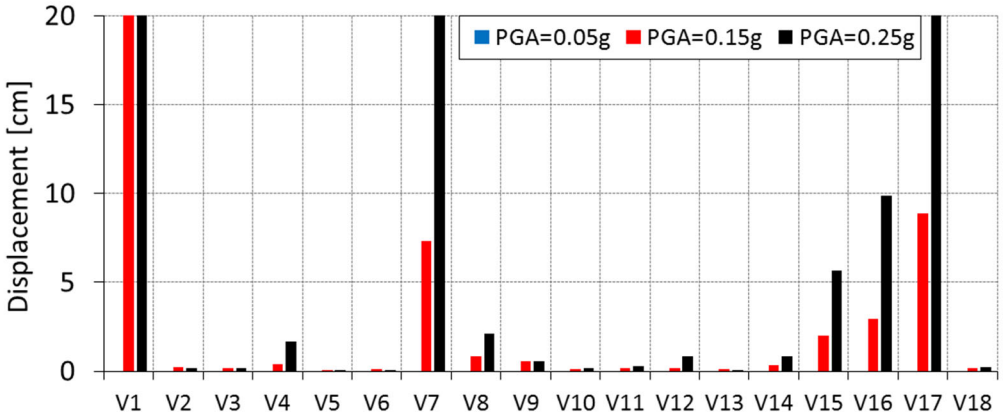

Fig. 22. Palazzo Te. Maximum vertical displacements registered for the main vaults during the non-linear dynamic analyses with different PGA.

5.2. Palazzo d'Arco

Fig. 23 shows the deformed shapes and the corresponding periods of the main vibration modes with participating mass ratio (PMR) larger than about 5% for Palazzo d'Arco: moreover, the distribution of the first three hundred modes in the two orthogonal directions is presented.

The first two main modes are Mode 2 (T=0.239 s) with the largest PMR (equal to 14.7%) in the Y direction, and Mode 7 (T=0.156 s) with PMR equal to 6.33% in the X direction: they both involve mainly the central block of the building. It can be noted that there is a large difference between the periods of the first two main modes. Other relevant modes are Mode 8 (T=0.155 s), involving mainly the left wing, and Mode 11 (T=0.145 s), involving the central block and the theatre: they both present a large PMR equal to 13.08% and 13.98%, respectively, in the Y direction. Mode 9 (T=0.153 s) and Mode 12 (0.142 s) involve mainly the exedra and the left and right wings, with a relevant PMR in the X direction. The first three hundred modes correspond to a total PMR of 85% for both the directions. It can be noted that the main vibration modes present a period corresponding to high amplifcations of the spectral accelerations, above all in the Y direction: the critical elements of the building result the central block, the exedra and the wings of the complex.

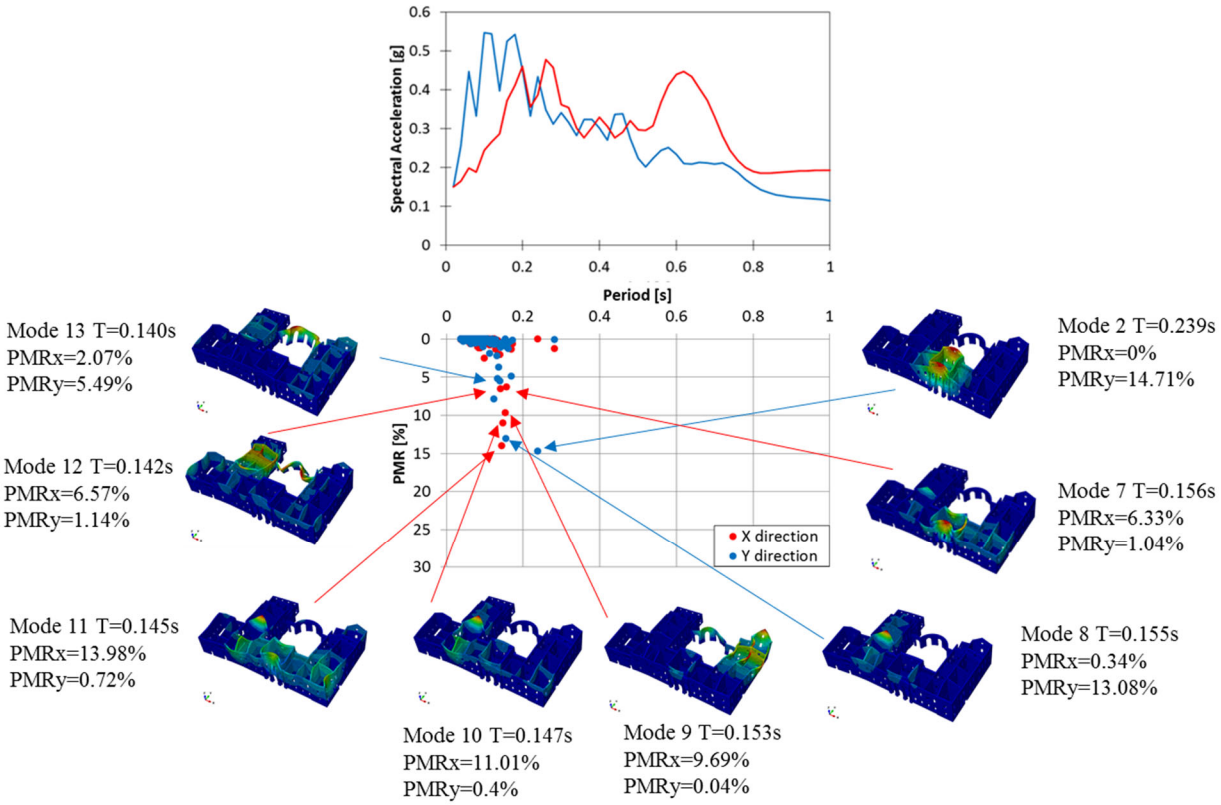

Fig. 23. Palazzo d'Arco. Distribution of the first three hundred modes in the X and Y directions. Deformed shapes and corresponding periods of the main vibration modes with indication of the participating mass ratios in the X and Y directions.

Fig. 24 and Fig. 25 show the tensile damage contour plots of Palazzo d'Arco at the end of the non-linear dynamic analyses with different PGA.

-The results of the non-linear dynamic analysis with PGA=0.05g highlight the onset of damage in the critical elements of the building. Visible damage can be observed along the corners of the walls and mainly in the central block and in the tympanum of the main façade. Evident damage is registered also in the exedra in correspondence with the large arches.

The numerical results confirm that the real damage observed in correspondence with the vaults of the greenhouse is due mainly to a poor interlocking between the perimeter walls and the vaults. In fact, the numerical model shows that a proper level of interlocking can prevent the formation of such cracks under PGA=0.05g. The numerical analyses with higher PGA values indicate that the vaults of the greenhouse are critical elements, showing cracks similar to those surveyed after the seismic sequence.

Moreover, it can be noted that in the numerical model the barrel and ribbed vaults of the first floor (towards the south side) present visible damage, as confirmed by the crack running the surface of the vault. Further damage is registered also in correspondence with some lintels in agreement with the damage survey, like the crack detected along the lintel of a door of the Green Room located at the first floor in the north part of the complex.

-The results of the non-linear dynamic analysis with PGA=0.15g show that the building exhibits widespread damage. The external and internal (towards the garden) walls present an onset of damage in correspondence with the openings at the ground and at the first levels, while the cracks are considerably marked along the corners of the walls. No visible damage is registered in the walls of the greenhouse, but significant damage can be observed in the vaults due to their small thickness and in the connection regions with the north-west wall. The other masonry vaults, located in the central part of the complex, present widespread damage over the whole surface.

-The numerical analyses show a significant increase of damage in the case of non-linear dynamic analysis with PGA=0.25g. The onset of damage observed in the external walls under PGA=0.15g considerably increases, presenting cracks in the spandrels, mainly in correspondence with the openings. Several walls show widespread inclined shear cracks originating from the corners of the openings. In correspondence with the corners of the walls there is evident damage caused by out-of-plane mechanisms and favored by the presence of openings and by the irregular plan configuration of the complex. The presence of irregularities in elevation, mainly in the south-west side, causes cracks in correspondence with the connection regions between two blocks with different heights.
The cross vaults of the greenhouse exhibit widespread damage in correspondence with the perimeter walls, presenting several cracks over the entire vaulted surface, similarly to the barrel and ribbed vaults of the central block.

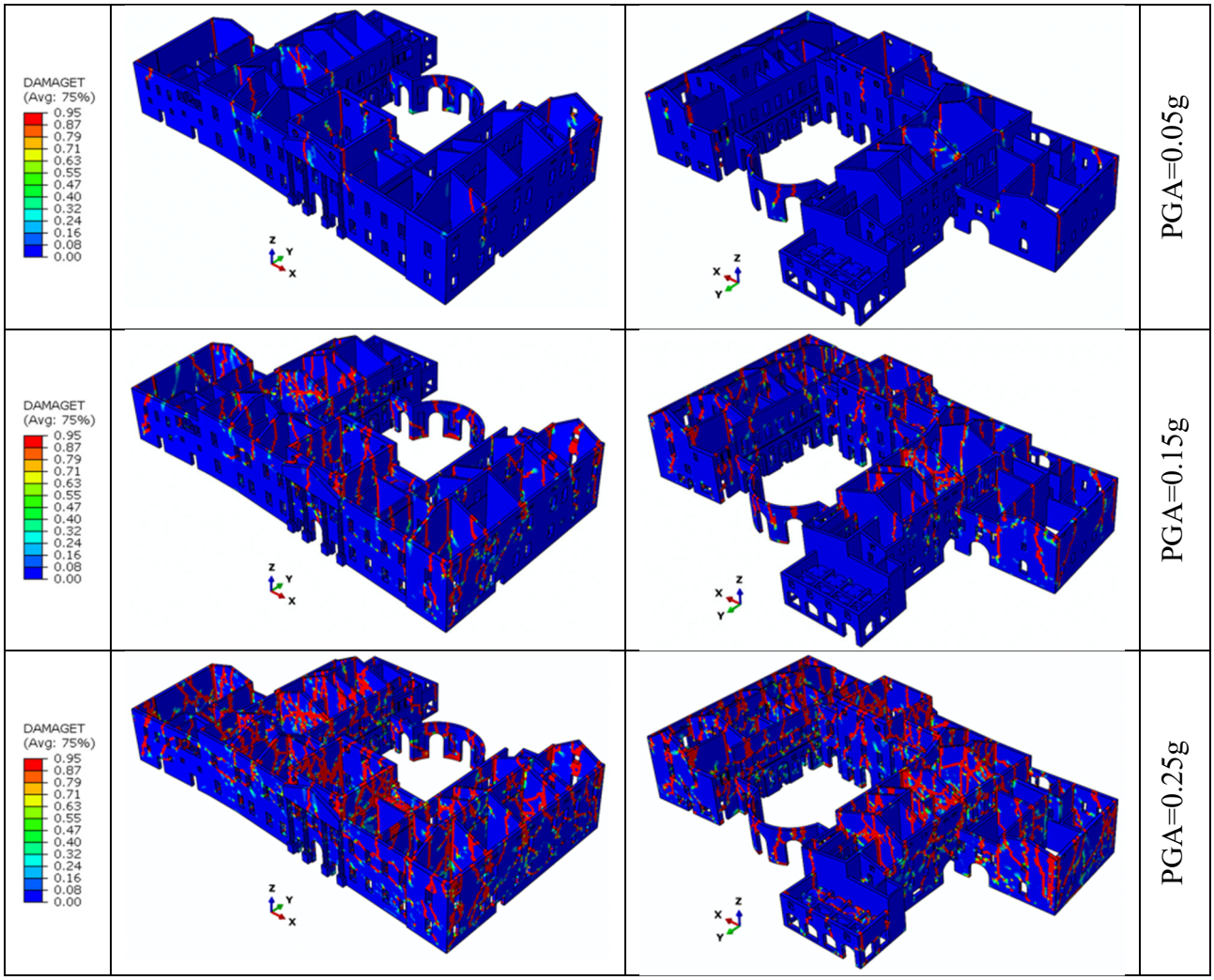

Fig. 24. Palazzo d'Arco. Tensile damage contour plot at the end of the non-linear dynamic analyses with different PGA: axonometric views.

	PGA=0.05g	PGA=0.15g	PGA=0.25g

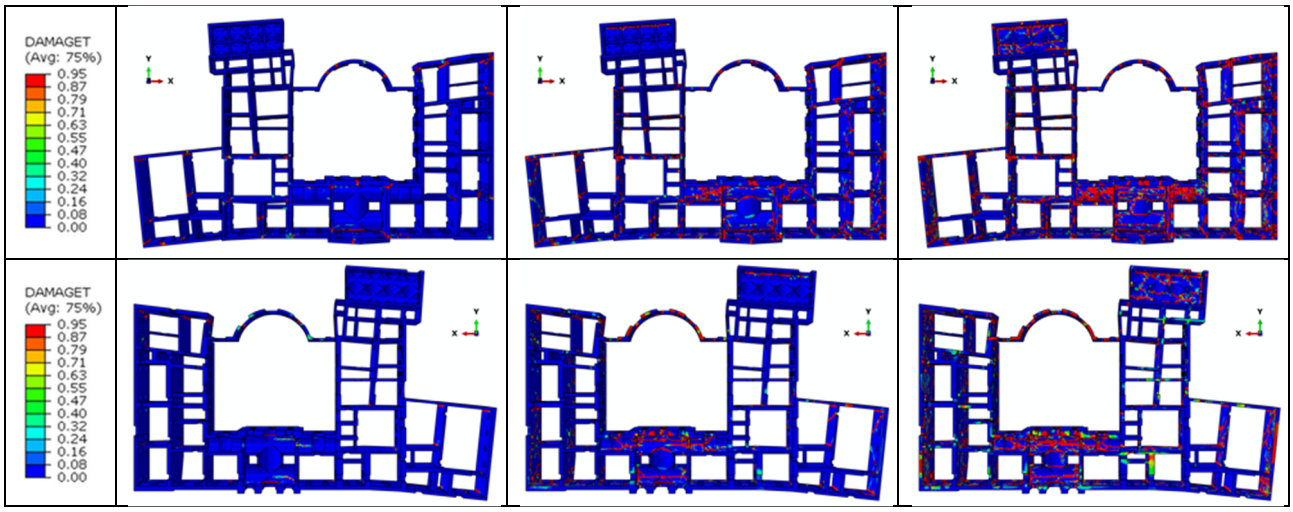

Fig. 25. Palazzo d'Arco. Tensile damage contour plot at the end of the non-linear dynamic analyses under different PGA: top and bottom views.

Fig. 26 shows the EDDTD values for the main macro-elements of Palazzo d'Arco at the end of the non-linear dynamic analyses with different PGA. The vaults of the entrance (V9 and V11) present the maximum values of EDDTD: the eight small vaults of the greenhouse show similar EDDTD values. As regards the walls, the central block (CB) presents the highest value of EDDTD. High EDDTD values are registered also for the exedra (E), the external north wall (ENW), the north-west wall (NWW) and the theatre (T).

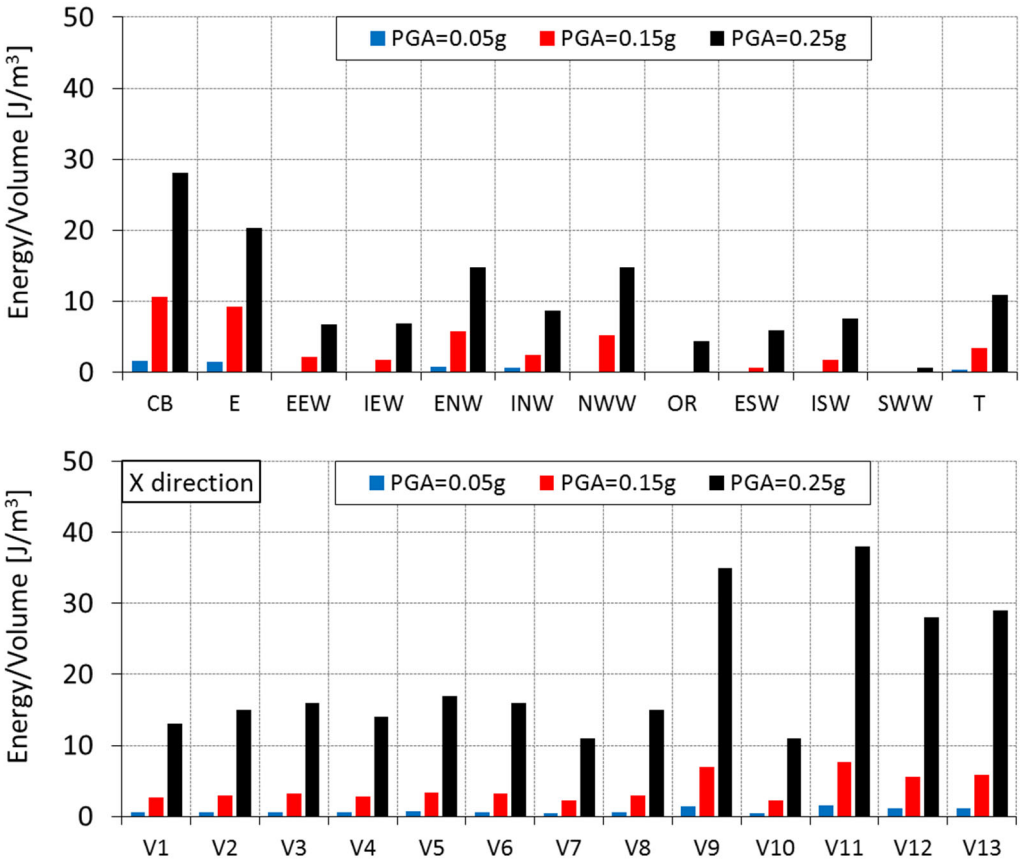

VS	VE				
V1-V8	V9	V10	V11	V12	V13

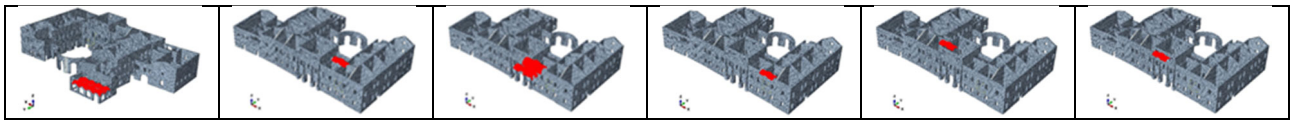

Fig. 26. Palazzo d'Arco. Energy density dissipated by tensile damage (EDDTD) for the main macro-elements at the end of the non-linear dynamic analyses with different PGA.

Fig. 27 shows the maximum normalized displacements (top displacement/height) registered in the X and Y directions for the main macro-elements of Palazzo d'Arco during the non-linear dynamic analyses with different PGA. The external north wall (ENW) presents the highest normalized displacement (1.8%) in the X direction: values larger than 1% are registered also for the internal south wall (ISW) and the theatre (T). Larger normalized displacements are generally registered in the Y direction: in fact, several walls present normalized displacements larger than 1.2%, such as the central block (CB), the exedra (E), the external east wall (EEW), the north-west wall (NWW) and the theatre (T).
Fig. 28 shows the maximum vertical displacements registered for the main vaults of Palazzo d'Arco during the non-linear dynamic analyses with different PGA. It can be noted that that the vaults of the entrance (V9-V11) present vertical displacements larger than 2.5 cm.

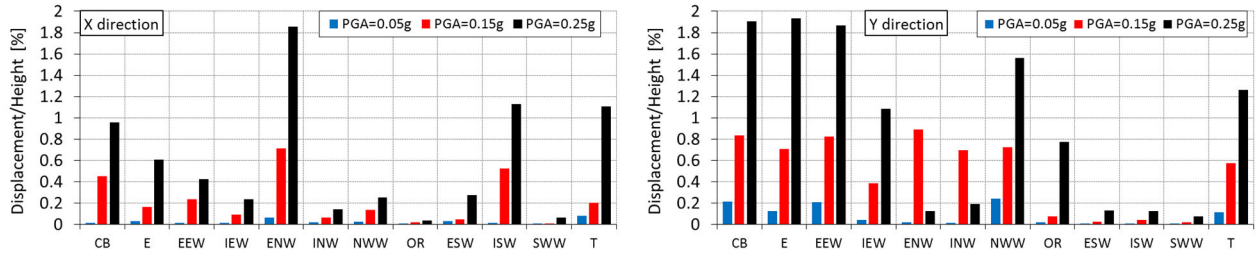

Fig. 27. Palazzo d'Arco. Maximum normalized displacements (top displacement/height) registered for the main macro-elements in the X and Y directions during the non-linear dynamic analyses with different PGA.

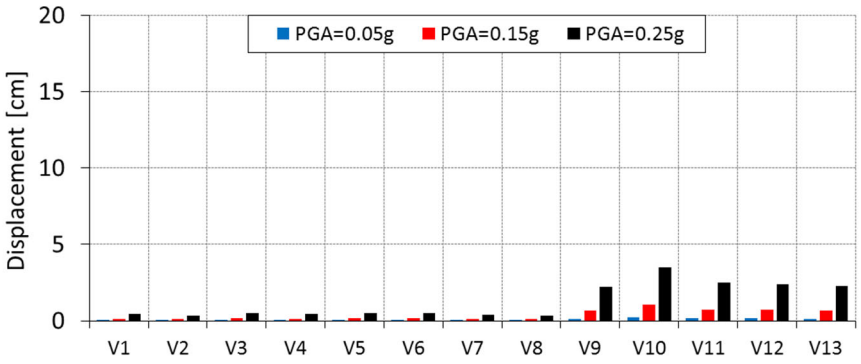

Fig. 28. Palazzo d'Arco. Maximum vertical displacements registered for the main vaults during the non-linear dynamic analyses with different PGA.

5.3. Palazzo dell'Accademia

Fig. 29 shows the deformed shapes and the corresponding periods of the main vibration modes with participating mass ratio (PMR) larger than 5% for Palazzo dell'Accademia: moreover, the distribution of the first three hundred modes in the two orthogonal directions is presented.
It can be noted that the first eight modes are characterized by PMR smaller than 5%: the first two main modes are Mode 9 (T=0.236 s), involving the south wall of the courtyard (SWC) and the wall separating the theatre and building (TBW) with PMR equal to 5.3% in the X direction, and Mode 10 (T=0.224 s), involving the west wall (WW) with PMR equal to 5.8% in the Y direction. Mode 14

(T=0.185 s) concerns mainly the east walls (EWC and EW) with PMR equal to 5.5% in the Y direction. In this case there is a notable difference between the periods of the second and third main modes. The most relevant modes are Mode 16 (T=0.176 s), involving the lateral walls along the Y direction with the largest PMR (27.5%) in the X direction and Mode 19 (T=0.166 s), involving a large part of the building with the largest PMR (7.7%) in the Y direction. The first three hundred modes correspond to a total PMR of 89% for both the directions.
It can be noted that the main vibration modes present a period corresponding to high amplifcations of the spectral accelerations: the external perimeter walls can be preliminarily considered the critical elements of the building.

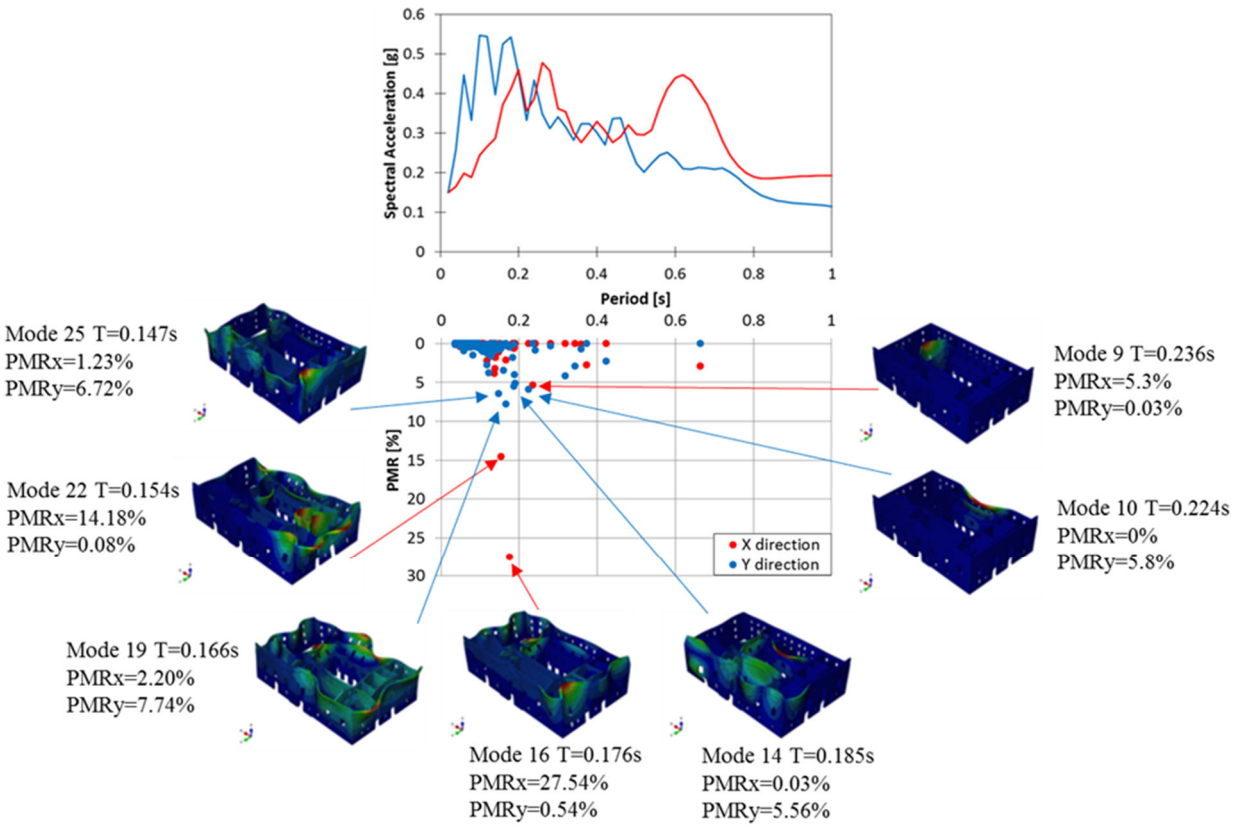

Fig. 29. Palazzo dell'Accademia. Distribution of the first three hundred modes in the X and Y directions. Deformed shapes and corresponding periods of the main vibration modes with indication of the participating mass ratios in the X and Y directions.

Fig. 30 and Fig. 31 show the tensile damage contour plots of Palazzo dell'Accademia at the end of the non-linear dynamic analyses with different PGA.
-The results of the non-linear dynamic analysis with PGA=0.05g show that the building presents an onset of damage in correspondence with the openings and the corners of the walls. A good correlation between numerical results and damage survey can be observed for the cross vaults of the first floor and the lintels of the doors (typical shear failure), such as the door of the historical archive at the second floor. Moreover, the numerical model shows a crack along the wall of the stair leading to the second floor in the north part of the building, as confirmed by the damage survey.
It is worth mentioning that no damage is registered in the numerical model along the wall dividing the "Staircase of Honour" and the library. This result confirms that the damage observed during the survey was due mainly to the thrust of a steel beam, which is not present in the numerical model.
-The results of the non-linear dynamic analysis with PGA=0.15g show that the whole building experiences extensive damage in the masonry walls and vaults. Cracks are concentrated mainly in correspondence with the corners of the building: vertical cracks above the lintels and X-shaped cracks

near the openings can be observed. Visible damage is detected in correspondence with the cross vaults of the Corridor of Honour at the first storey.
-The results of the non-linear dynamic analysis with PGA=0.25g show a large increase of damage in the whole building. The damage observed along the corners of the complex is much marked: significant damage concentration, which is mainly due to the absence of orthogonal walls and slabs, may be observed in correspondence with the upper part of the corner between the north and east walls and along the height of the corner between the west and south walls. A series of cracks can be registered in correspondence with a "veletta" of small thickness and relevant height, which is located in the upper part of the north and east walls: such cracks propagate along the remaining part of the wall involving the openings.
The presence of several openings significantly decreases the strength of the perimeter walls, causing widespread X-shaped cracks near the openings and triggering shear failure mechanisms of the walls: it can be noted that the cracks generally originate from the corners of the openings.
Widespread damage can be observed in the cross vaults and in the concrete-masonry slab located in the west part and partially in the north and east parts of the building.

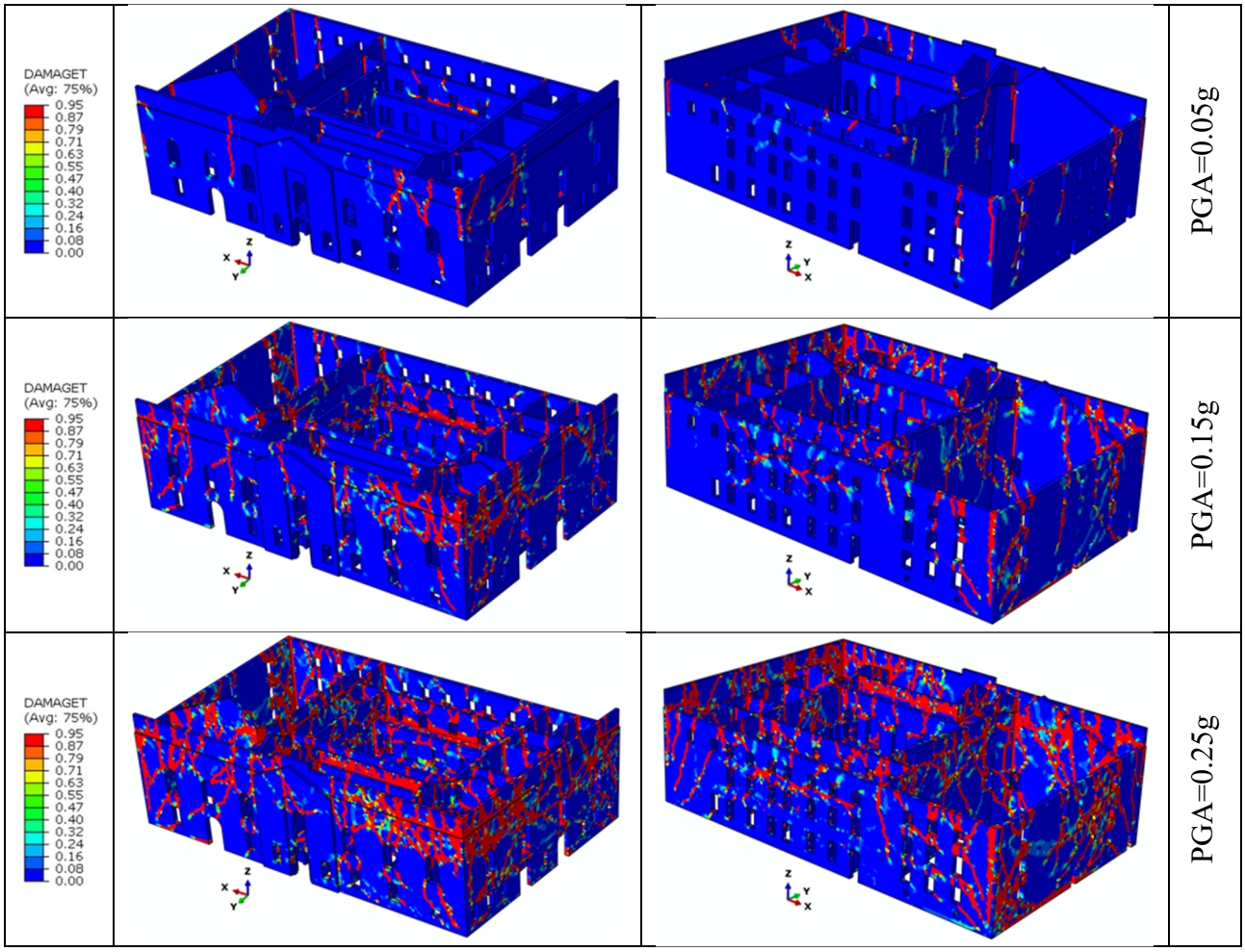

Fig. 30. Palazzo dell'Accademia. Tensile damage contour plot at the end of the non-linear dynamic analyses with different PGA: axonometric views.

	PGA=0.05g	PGA=0.15g	PGA=0.25g

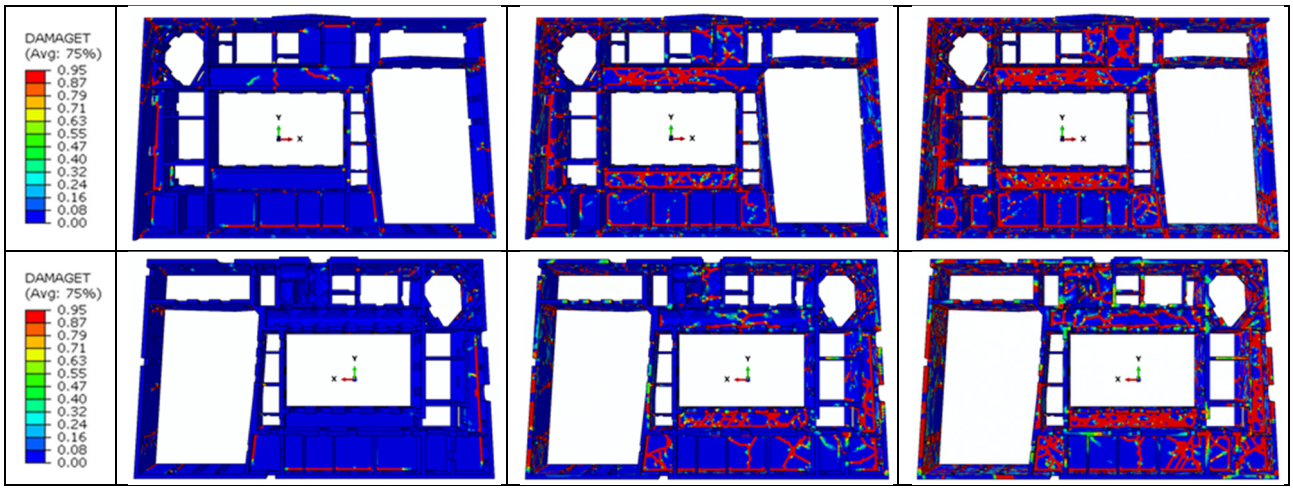

Fig. 31. Palazzo dell'Accademia. Tensile damage contour plot at the end of the non-linear dynamic analyses with different PGA: top and bottom views.

Fig. 32 shows the EDDTD values for the main macro-elements of Palazzo dell'Accademia at the end of the non-linear dynamic analyses with different PGA. The vaults of the corridor at the first floor (VC1) present the highest values of EDDTD: high EDDTD values are registered also for the vaults of the staircase (VS). As regards the walls, the north wall (NW) presents the highest value of EDDTD: high EDDTD values are registered also for the east wall (EW), the south wall (SW), the wall separating the theatre and building (TBW).

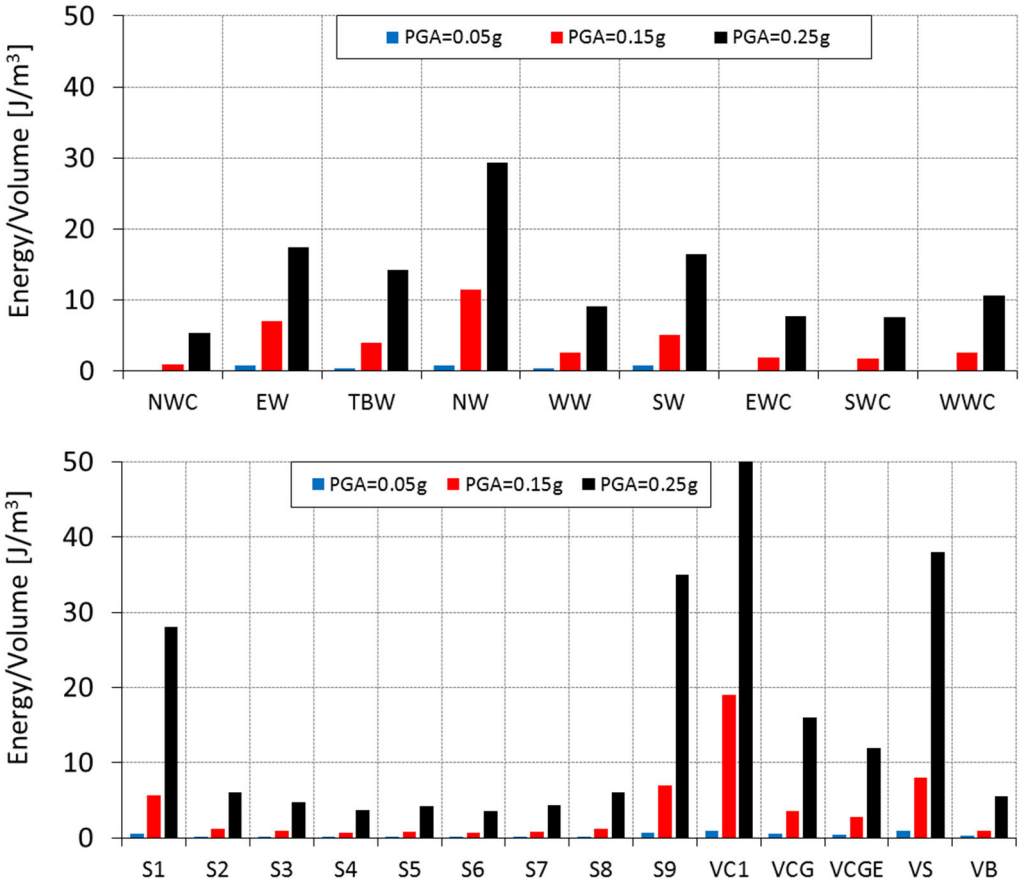

S1-S8	S9	VC1	VCG-VCGE	VS	VB

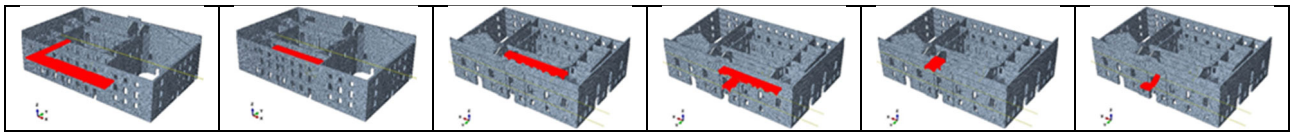

Fig. 32. Palazzo dell'Accademia. Energy density dissipated by tensile damage (EDDTD) for the main macro-elements at the end of the non-linear dynamic analyses with different PGA.

Fig. 33 shows the maximum normalized displacements (top displacement/height) registered in the X and Y directions for the main macro-elements of Palazzo dell'Accademia during the non-linear dynamic analyses with different PGA. The north wall (NW) presents the largest normalized displacement (about 3.5%) in the X direction. Normalized displacements larger than 1.2% are registered also for the wall separating the theatre and the building (TBW) and the south wall (SW).
In the Y direction, the largest normalized displacement (about 1.6%) is registered for the east wall (EW): high values (larger than 1.2%) are observed for the west wall of the courtyard (WWC) and the west wall (WW).
Fig. 34 shows the maximum vertical displacements registered for the main slabs and vaults during the non-linear dynamic analyses with different PGA. It can be noted that the vaults of the corridor at the first floor (VC1) present vertical displacements equal to about 3 cm: the maximum vertical displacements (larger than 13 cm) are registered for slabs S1 and S9 that are characterized by an elongated shape.

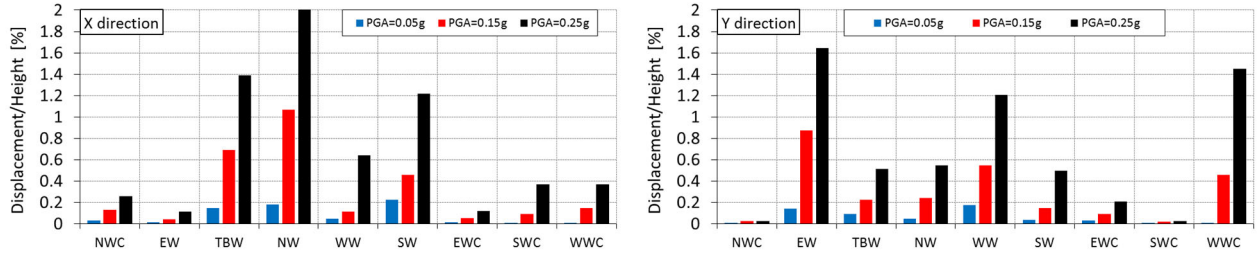

Fig. 33. Palazzo dell'Accademia. Maximum normalized displacements (top displacement/height) registered for the main macro-elements in the X and Y directions during the non-linear dynamic analyses with different PGA.

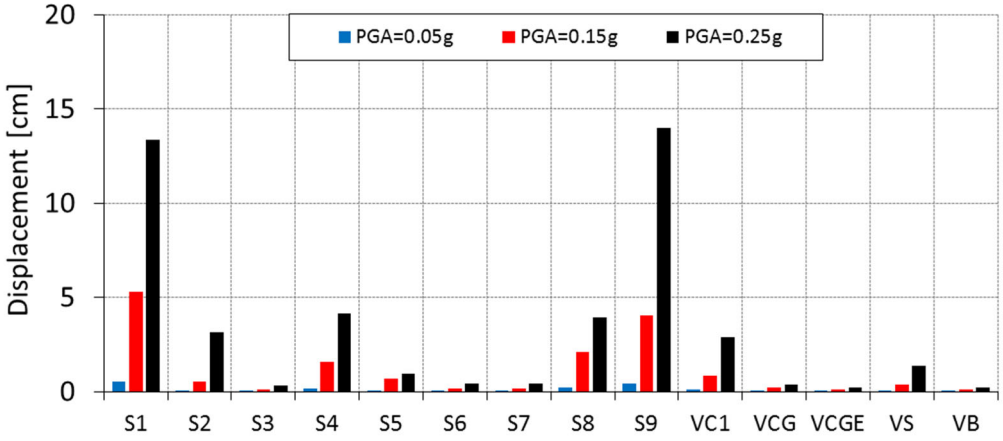

Fig. 34. Palazzo dell'Accademia. Maximum vertical displacements registered for the main slabs and vaults during the non-linear dynamic analyses with different PGA.

6. Comparison of the numerical results

-The results of the eigen-frequency analyses show that all the buildings present low values of periods for the most relevant modes (with high participating mass ratio) and consequently high amplifications of spectral accelerations are expected for such a typology of structures. It is important to observe that the eigen-frequency analysis provides a preliminary rough indication of the critical elements for each building, which are in a good agreement with the following results obtained through non-linear dynamic analyses.

-Fig. 35 shows the total energy and the total energy density dissipated by tensile damage (EDTD and EDDTD, respectively) for the three buildings at the end of the non-linear dynamic analyses with different PGA. It can be noted that the highest EDTD value is computed for Palazzo Te due to its large volume: conversely, the highest EDDTD value is registered for Palazzo dell'Accademia for all the PGA considered. Similar EDDTD values are observed for Palazzo Te and Palazzo d'Arco, for PGA=0.05g and PGA=0.15g: however, Palazzo Te shows the lowest EDDTD value under PGA=0.25g.

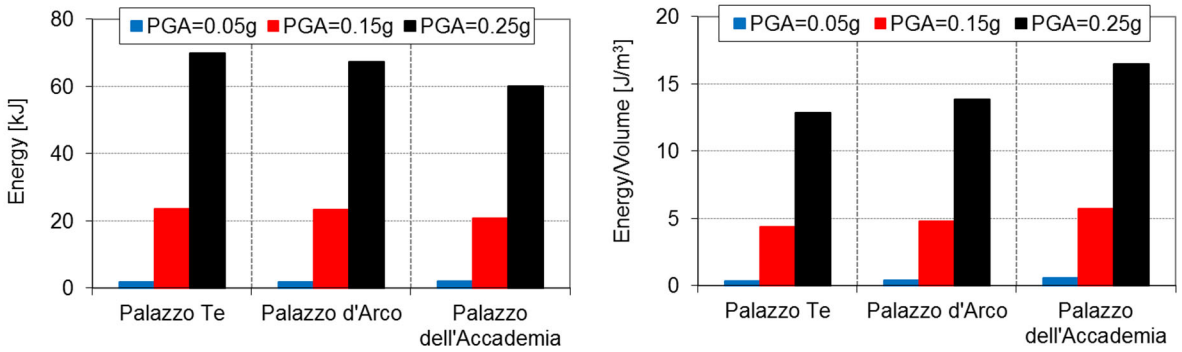

Fig. 35. Total energy (EDTD) and total energy density (EDDTD) dissipated by tensile damage for the different buildings at the end of the non-linear dynamic analyses with different PGA.

-The vaults are the most damaged elements for all the buildings: the highest EDDTD value is registered for the vaults of the corridor at the first floor (VC1) of Palazzo dell'Accademia and for the east vaults (VE) of Palazzo Te. Palazzo d'Arco shows the smallest peak values of vertical displacements. Moreover, it can be noted that Palazzo Te presents a more uniform damage distribution in the walls than the other buildings, showing the lowest EDDTD values for the vertical elements. Palazzo d'Arco and Palazzo dell'Accademia show similar EDDTD values for the vertical elements. The most damaged vertical elements are the external north wall (WNE) for Palazzo Te, the central block (CB) and the exedra (E) for palazzo d'Arco, the east wall or façade (EW) for Palazzo dell'Accademia.

-The maximum values of the normalized horizontal displacements are registered for the lateral external walls for all the buildings. Palazzo Te shows the highest values of normalized displacements for the external north wall (WNE) in the X direction and for the wall of the Loggia (WL) in the Y direction. As regards Palazzo d'Arco, the maximum values of normalized displacements are registered for the external north wall (ENW) in the X direction and for the exedra (E) in the Y direction. Palazzo dell'Accademia exhibits the maximum values of normalized displacements for the north wall (NW) in the X direction and for the east wall (EW) in the Y direction.
It is interesting to observe that the maximum normalized displacements in the two orthogonal directions are similar for Palazzo d'Arco, while there is a large difference for Palazzo Te and Palazzo dell'Accademia due to the high values computed for the two weak parts (the external north wall (WNE) for Palazzo Te and the north wall (NW) for Palazzo dell'Accademia).

-Palazzo Te shows the largest vertical displacements among the three buildings: they are registered for the west vaults (VW). Significant vertical displacements are also observed for the east vault (VE), as confirmed by the high EDDTD values. Palazzo d'Arco and Palazzo dell'Accademia exhibit smaller vertical displacements of the vaults than Palazzo Te.

7. Conclusions

This paper has described the main damage occurred in three important historical buildings of the outstanding cultural heritage in Mantua during the recent Emilia seismic sequence: then, the seismic response of the three palaces has been investigated through advanced numerical simulations carried out on detailed FE models using a damage plasticity model with different softening behavior in tension and compression for masonry.

-The damages suffered by the buildings during the 2012 Emilia earthquake have shown the poor seismic behavior of such a typology of structures even under low seismic actions. Visual inspections and photographic collections have highlighted the most vulnerable elements and the critical parts of the buildings under study. In particular, significant cracks were observed in correspondence with the masonry walls and vaults with severe damage to the decorations, in the connection regions between the vaults and the perimeter walls: further cracks were registered in the lintels of doors, near the windows and along the corners of masonry walls.

- The available information and data collected from field surveys and documentary research have provided a preliminary knowledge of great importance for developing detailed FE models of the structures and for better understanding the results of advanced numerical simulations.

- A good correlation between numerical results and real damage has been observed in this study. The results of the non-linear dynamic analyses with low PGA show that the cracks patterns observed in the buildings after the 2012 Emilia earthquake can be simulated satisfactorily by the numerical approach adopted.

-The numerical simulations have provided a deep insight into the seismic behavior of the buildings for different seismic intensity levels. In particular, the non-linear dynamic analyses have given a proper indication of the damage distribution and the most vulnerable parts of the buildings for higher PGA values than those registered in Mantua during the 2012 Emilia earthquake.

-The numerical results have highlighted extensive damage in the vaults, which are the critical elements for all the buildings: the highest EDDTD values are registered for the vaults of the corridor at the first floor (VC1) of Palazzo dell'Accademia and for the east and west vaults (VE and VW) of Palazzo Te. The analysis of the vertical displacements show the probable collapse of the west vaults (VW) of Palazzo Te.

-The maximum values of the normalized horizontal displacements are registered for the external walls for all the three buildings. The critical elements for each building are: (1) the external north wall (WNE) for Palazzo Te; (2) the external north wall (ENW), the central block (CB) and the exedra (E) for Palazzo d'Arco; (3) the façade (EW) and the north wall (NW) for Palazzo dell'Accademia.

References

[1] D'Ayala DF, Paganoni S. Assessment and analysis of damage in L'Aquila historic city centre after 6th April 2009. Bulletin of Earthquake Engineering 2011;9(1):81-104.

[2] Valente M, Milani G. Seismic response and damage patterns of masonry churches: seven case studies in Ferrara, Italy. Engineering Structures 2018, 177.

[3] Lucibello G, Brandonisio G, Mele E, De Luca A. Seismic damage and performance of Palazzo Centi after L'Aquila earthquake: A paradigmatic case study of effectiveness of mechanical steel ties. Engineering Failure Analysis 2013;34:407-430.

[4] Ceci AM, Contento A, Fanale L, Galeota D, Gattulli V, Lepidi M, Potenza F. Structural performance of the historic and modern buildings of the University of L'Aquila during the seismic events of April 2009. Engineering Structures 2010;32(7):1899-1924.

[5] Clementi F, Pierdicca A, Formisano A, Catinari F, Lenci S. Numerical model upgrading of a historical masonry building damaged during the 2016 Italian earthquakes: the case study of the Podestà palace in Montelupone (Italy). Journal of Civil Structural Health Monitoring 2017;7(5):703-717.

[6] Lourenço PB, Nuno Mendes AT, Ramos LF. Seismic performance of the St. George of the Latins church: lessons learned from studying masonry ruins. Eng. Struct 2012;40:501-518.

[7] Criber, E., G. Brando, and G. De Matteis. The effects of L'Aquila earthquake on the St. Gemma church in Goriano Sicoli: part I-damage survey and kinematic analysis. Bulletin of Earthquake Engineering 2015;13(12):3713-3732.

[8] Ascione F, Ceroni F, De Masi RF, De Rossi F, Pecce MR. Historical buildings: Multidisciplinary approach to structural/energy diagnosis and performance assessment. Applied Energy 2017;185:1517-1528.

[9] Aras F, Altay G. Seismic evaluation and structural control of the historical Beylerbeyi Palace. Structural Control and Health Monitoring 2015;22(2):347-364.

[10] Ceroni F, Sica S, Pecce MR, Garofano A. Evaluation of the natural vibration frequencies of a historical masonry building accounting for SSI. Soil Dynamics and Earthquake Engineering 2014;64:95-101.

[11] El-Borgi S, Smaoui H, Casciati F, Jerbi K, Kanoun F. Seismic evaluation and innovative retrofit of a historical building in Tunisia. Structural Control and Health Monitoring 2005;12(2):179-195.

[12] Gattulli V, Lofrano E, Paolone A, Pirolli G. Performances of FRP reinforcements on masonry buildings evaluated by fragility curves. Computers & Structures 2017;190:150-161.

[13] Barbieri G, Valente M, Biolzi L, Togliani C, Fregonese L, Stanga G. An insight in the late Baroque architecture: an integrated approach for a unique Bibiena church. Journal of Cultural Heritage 2017;23:58-67.

[14] Krstevska L, Tashkov L, Naumovski N, Florio G, Formisano A, Fornaro A, Landolfo R. In-situ experimental testing of four historical buildings damaged during the 2009 L'Aquila earthquake. COST ACTION C26: Urban Habitat Constructions under Catastrophic Events – Proceedings of the Final Conference, 2010. pp. 427-432.

[15] Roca P, Cervera M, Gariup G. Structural analysis of masonry historical constructions. Classical and advanced approaches. Archives of Computational Methods in Engineering 2010;17(3):299-325.

[16] Endo Y, Pelà L, Roca P, Da Porto F, Modena C. Comparison of seismic analysis methods applied to a historical church struck by 2009 L'Aquila earthquake. Bulletin of Earthquake Engineering 2015;13(12):3749-3778.

[17] Castori G, Borri A, De Maria A, Corradi M, Sisti R. Seismic vulnerability assessment of a monumental masonry building. Engineering Structures 2017;136:454-465.

[18] Formisano A, Marzo A. Simplified and refined methods for seismic vulnerability assessment and retrofitting of an Italian cultural heritage masonry building. Computers & Structures 2017;180:13-26.

[19] Hadzima-Nyarko M, Mišetić V, Morić D. Seismic vulnerability assessment of an old historical masonry building in Osijek, Croatia, using Damage Index. Journal of Cultural Heritage 2017;28:140-150.

[20] Sandoval C, Valledor R, Lopez-Garcia D. Numerical assessment of accumulated seismic damage in a historic masonry building. A case study. International Journal of Architectural Heritage 2017;11(8):1177-1194.

[21] Betti M, Bartoli G, Orlando M. Evaluation study on structural fault of a Renaissance Italian palace. Engineering Structures 2010;32(7):1801-1813.

[22] Ceroni F, Pecce MR, Sica S, Garofano A. Assessment of seismic vulnerability of a historical masonry building. Buildings 2012;2(3):332-358.

[23] Milani G, Shehu R, Valente M. Possibilities and limitations of innovative retrofitting for masonry churches: Advanced computations on three case studies. Construction and Building Materials 2017:147;239-263.

[24] Milani G, Shehu R, Valente M. A kinematic limit analysis approach for seismic retrofitting of masonry towers through steel tie-rods. Engineering Structures 2018;160:212-228.

[25] Formisano A, Florio G, Landolfo R, Mazzolani FM. Numerical calibration of a simplified procedure for the seismic behaviour assessment of masonry building aggregates. In: Proceedings of the 13th International Conference on Civil, Structural and Environmental Engineering Computing; 2011.

[26] Formisano A. Theoretical and numerical seismic analysis of masonry building aggregates: case studies in San Pio Delle Camere (L'Aquila, Italy). Journal of Earthquake Engineering 2017;21(2):227-245.

[27] Clementi F, Gazzani V, Poiani M, Lenci S. Assessment of seismic behaviour of heritage masonry buildings using numerical modelling. Journal of Building Engineering 2016;8: 29-47.

[28] Clementi F, Gazzani V, Poiani M, Mezzapelle PA, Lenci S. Seismic assessment of a monumental building through nonlinear analyses of a 3D solid model. Journal of Earthquake Engineering 2018;Supp.1:35-61.

[29] Lourenço PB, Nuno Mendes AT, Ramos LF. Seismic performance of the St. George of the Latins church: lessons learned from studying masonry ruins. Eng. Struct. 2012;40:501-518.

[30] Betti M, Galano L. Seismic analysis of historic masonry buildings: the vicarious palace in Pescia (Italy). Buildings 2012;2(2):63-82.

[31] Valente M, Milani G. Effects of geometrical features on the seismic response of historical masonry towers. Journal of Earthquake Engineering 2018, Supp 1, 2-34.

[32] Milani G, Valente M, Alessandri C. The narthex of the Church of the Nativity in Bethlehem: a non-linear finite element approach to predict the structural damage. Computers & Structures 2018;207:3-18.

[33] Penna A, Morandi P, Rota M, Manzini CF, Da Porto F, Magenes G. Performance of masonry buildings during the Emilia 2012 earthquake. Bulletin of Earthquake Engineering 2014;12(5):2255-2273.

[34] Sorrentino L, Liberatore L., Decanini LD, Liberatore D. The performance of churches in the 2012 Emilia earthquakes. Bulletin of Earthquake Engineering 2013;12:2299-2331.

[35] Valente M, Barbieri G, Biolzi L. Seismic assessment of two masonry Baroque churches damaged by the 2012 Emilia earthquake. Engineering Failure Analysis 2017;79:773-802.

[36] Valente M, Milani G. Damage survey, simplified assessment, and advanced seismic analyses of two masonry churches after the 2012 Emilia earthquake. International Journal of Architectural Heritage 2018. https://doi.org/10.1080/15583058.2018.1492646.

[37] Valente M, Milani G. Damage assessment and partial failure mechanisms activation of historical masonry churches under seismic actions: Three case studies in Mantua. Engineering Failure Analysis 2018;92:495-519.

[38] Barbieri G, Biolzi L, Bocciarelli M, Fregonese L, Frigeri A. Assessing the seismic vulnerability of a historical building. Engineering Structures 2013;57:523-535.

[39] ABAQUS®, Theory Manual, Version 6.14.

[40] Lubliner J, Oliver J, Oller S, Oñate E. A plastic-damage model for concrete (1989). International Journal of Solids and Structures 1989;25:299-326.

[41] Lee J, Fenves GL. Plastic-Damage Model for Cyclic Loading of Concrete Structures (1998). Journal of Engineering Mechanics 1998;124:892-900.

[42] Van Der Pluijm R. (1993). Shear Behaviour of bed joints. Proceedings of 6th North American masonry conference, Philadelphia, 125-136

[43] Page A. The biaxial compressive strength of brick masonry. Proceedings of the Institute of Civil Engineering 1981;871-893

[44] DM 14/01/2008. Nuove norme tecniche per le costruzioni. Ministero delle Infrastrutture (GU n.29 04/02/2008), Rome, Italy. [New technical norms on constructions].

[45] Circolare n° 617 del 2 febbraio 2009. Istruzioni per l'applicazione delle nuove norme tecniche per le costruzioni di cui al decreto ministeriale 14 gennaio 2008. [Instructions for the application of the new technical norms on constructions].

[46] DPCM 9/2/2011. Linee guida per la valutazione e la riduzione del rischio sismico del patrimonio culturale con riferimento alle Norme tecniche delle costruzioni di cui al decreto del Ministero delle Infrastrutture e dei trasporti del 14 gennaio 2008. [Italian guidelines for the evaluation and the reduction of the seismic risk for the built heritage, with reference to the Italian norm of constructions].